UNIVERSITY OF TURKISH AERONAUTICAL ASSOCIATION
INSTITUTE OF SCIENCES AND TECHNOLOGY

FRACTAL MICROSTRIP FILTER FOR WIRELESS COMMUNICATIONS

MASTER THESIS

Hiba Hashim SALEH

Department of Electrical and Electronics Engineering

Master Thesis Program

NOVEMBER 2017

UNIVERSITY OF TURKISH AERONAUTICAL ASSOCIATION
INSTITUTE OF SCIENCES AND TECHNOLOGY

FRACTAL MICROSTRIP FILTER FOR WIRELESS COMMUNICATIONS

MASTER THESIS

Hiba Hashim SALEH

1406030031

Department of Electrical and Electronics Engineering

Master Thesis Program

Thesis Supervisor: Asst. Prof. Dr. Özgür KELEKÇİ

Hiba Hashim Saleh, having student number 1406030031 and enrolled in the Master Program at the Institute of Science and Technology at the University of Turkish Aeronautical Association, after meeting all of the required conditions contained in the related regulations, has successfully accomplished, in front of the jury, the presentation of the thesis prepared with the title of: "**FRACTAL MICROSTRIP FILTERS FOR WIRELESS COMMUNICATIONS**"

Thesis Supervisor: Asst. Prof.Dr.Özgür KELEKÇİ
University of Turkish Aeronautical Association

Jury Member : Assoc.Prof.Dr.Mehmet ÜNLÜ
Yıldırım Beyazıt University

:Asst. Prof.Dr.Ertan ZENCİR
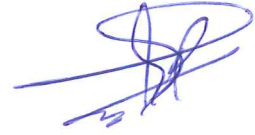University of Turkish Aeronautical Association

: Asst. Prof.Dr.Özgür KELEKÇİ
University of Turkish Aeronautical Association

Thesis Defense Date: 29. 11. 2017

**UNIVERSITY OF TURKISH AERONAUTICAL ASSOCIATION
TO THE INSTITUTE OF SCIENCES AND TECHNOLOGY**

I hereby declare that all information in this study I presented as my Master's Thesis, called "Fractal Microstrip Filters For Wireless Communications", has been presented in accordance with the academic rules and ethical conduct. I also declare and certify with my honor that I have fully cited and referenced all the sources I made use of in this present study.

29.11.2017

Hiba Hashim Saleh

ACKNOWLEDGEMENTS

CONTENTS

LIST OF TABLES

LIST OF FIGURES

ABBREVIATIONS

ADS	**:**	Advanced Design System
BP	**:**	Band Pass
BPF	**:**	Band Pass Filter
CRLH	**:**	Composite Right/Left-Handed
FBW	**:**	Fractional Bandwidth
IEEE	**:**	Institute of Electrical and Electronics Engineers
LP	**:**	Low Pass
LPF	**:**	Low Pass Filter
MAC	**:**	Media Access Control
MIC	**:**	Microwave Integrated Circuit
MMIC	**:**	Monolithic Microwave Integrated Circuit
RF	**:**	Radio Frequency
SIRs	**:**	Stepped Impedance Resonators
SLSIRs	**:**	Stub-Loaded Step Impedance Resonators
TEM	**:**	Transverse Electromagnetic Mode
TL	**:**	Transmission Line
UIR	**:**	Uniform Impedance Resonator
Wi-Fi	**:**	Wireless Fidelity
WLAN	**:**	Wireless Local Area Network

LIST OF SYMBOLS

C_p	:	Parallel LC resonator in the bandpass filter
C_s	:	Series LC resonator in the bandpass filter
C	:	Velocity of light in free space
D	:	Distance between coupling resonators
G	:	Conductance
g_0	:	Conductance or source resistance
g_n	:	Series inductance or the shunt capacitance
g_{n+1}	:	Load conductance or the load resistance
H	:	Thickness of the dielectric substrate
L_p	:	Parallel LC resonator in the bandpass filter
L_s	:	Series LC resonator in the bandpass filter
L_R	:	Return loss
L	:	Physical length of the microstrip
l_L	:	Physical length of high impedance line
l_C	:	Physical length of low impedance line
M_{ij}	:	Coupling coefficient
q_{ei}	:	Quality factor
R	:	Resistance
R_z	:	Ratio between two transmission line impedances
S	:	Space between conductors in the coupling microstrip line
T	:	Thickness of the conductor strip
v_p	:	Phase velocity
W	:	Width of conductor in microstrip line
ω_0	:	Angular resonator frequency
ω_c	:	Cutoff frequency
Y_0	:	Characteristic admittance
Y_1	:	Characteristic admittance of the first transmission line
$J_{j,j+1}$	:	Characteristic admittances of J-inverters
Z_0, Z_c	:	Characteristic impedance
Z_{0e}	:	The even-mode characteristic impedance
Z_{0C}	:	Characteristic impedances of the low impedance line
Z_{0L}	:	Characteristic impedances of the high impedance line
Z_{0o}	:	The odd-mode characteristic impedance
Z_1	:	Characteristic impedance of the first transmission line
Z_2	:	Characteristic impedance of the second transmission line
θ	:	Electrical length
θ_1	:	Electrical length of the first transmission line

θ_2	:	Electrical length of the second transmission line
f_0	:	Fundamental resonant frequency
λ_0	:	The free space wavelength
λ_{g0}	:	Guided wavelength
$\lambda_{g0}/4$	:	Quarter wavelength
$\lambda_{g0}/2$	:	Half-wavelength
ε_r	:	Relative dielectric constant
ε_{re}	:	Effective dielectric constant
η	:	The wave impedance in free space
β	:	Propagation constant
Ω_c	:	Cutoff angular frequency
A	:	Ratio length of the θ_2 to the physical length of SIR

ABSTRACT

FRACTAL MICROSTRIP FILTER FOR WIRELESS COMMUNICATIONS

SALEH, Hiba Hashim

Master Thesis, Department of Electrical and Electronics Engineering

Thesis Supervisor: Asst. Prof. Dr. Özgür KELEKÇİ

NOVEMBER 2017, 54 pages

This study presents new microstrip devices as bandpass and bandstop filters. The proposed filters use slotted patch microstrip resonator based on quasi fractal geometry, simulated by AWR_{12} software package. Both filters have quasi elliptic frequency response, were designed at centre frequency of 7.45 GHz and 6.02 GHz for bandpass filter and bandstop filter, respectively. FR4 and RT/Duroid substrates were used in the design of filters. Simulation results show that the designed quasi fractal bandpass filter has very narrow fractional bandwidth of 1.25 %which is very rare in microstrip filter design. This narrow band filter is useful in wireless schemes that require prevention of signals in very adjacent bands. On the other hand, the projected bandstop filter offers narrow rejection band that is useful in broadband wireless schemes influencing from fixed interferences. For RT/Duroid 6010.2 lm substrate, the projected quasi fractal BPF is designed at centre frequency of 2.505 GHz, while quasi fractal multi band BSF is designed at band frequencies of 2.5, 4.14 and 5.79 GHz respectively. The presented quasi fractal BPF has extremely narrow fractional bandwidth of 0.419%, which is tentatively amazing and ultra narrow band in microstrip filter design. On the other hand, quasi fractal BSF can be integrated within broadband wireless systems that are receptive to permanent frequency interferences for ISM and C band wireless applications. The measured frequency responses are in good agreement with the simulations. All filters have satisfactory

S_{11} and S_{21} responses besides smallness properties that stand for interesting features of the newest wireless applications. The simulated and measured frequency responses for all designed filters are in fine agreement with acceptable discrepancy.

Key words: Quasi Fractal Geometry, Microstrip Filters, Filter Smallness, Narrowband Frequency Responses.

ÖZET

KABLOSUZ ILETIŞIM IÇIN FRAKTAL MIKRO ŞERIT FILTRELER

SALEH, Hiba Hashim

Yüksek Lisans Tezi, Elektrik-Elektronik Anabilim Dalı

Tez Danışmanı: Yrd. Doç. Dr. Özgür KELEKÇİ

KASIM 2017, 54 sayfa

Bu tezde, bant geçiren ve bant durdurucu filtreler olarak yeni mikro şerit cihazları sunmaktadır. Önerilen filtreler, AWR12 yazılım paketi ile taklit edilen yarı fraktal geometriye dayanan yivli yama mikro şerit rezonatörünü kullanmaktadır. Her iki filtrenin, band geçişi filtresinde 7.45 GHz merkez frekansında ve bant derinliği filtresinde sırasıyla 6.02 GHz frekans bandında tasarlanan, eliptik frekans tepkisi vardır. Filtrelerin tasarımında kullanılan substrat özellikleri 4.4 dielektrik sabiti ve 1.5 mm dielektrik kalınlığıdır. Simülasyon sonuçları, tasarlanan yarı fraktal bant geçiren filtrenin, %1.25'lik çok dar kesirli bant genişliğine sahip olduğunu göstermektedir; bu, mikrodizge filtre tasarımında çok nadir görülür. Bu dar bant filtresi, çok bitişik bantlardaki sinyallerin önlenmesi gereken kablosuz şemalarda faydalıdır. Öte yandan, öngörülen bant durdurucu filtre, sabit girişimlerden etkileyen geniş bant kablosuz iletişim şemalarında yararlı olan dar reddi bandı sunar. RT / Duroid 6010.2 lm için, projelenmiş yarı fraktal BPF 2.505 GHz merkez frekansında, kısmi fraktal çok band BSF ise sırasıyla 2.5, 4.14 ve 5.79 GHz bant frekanslarında tasarlanmıştır. Sunulan yarı fraktal BPF, geçici olarak şaşırtıcı olan ve mikro şerit filtre tasarımında ultra dar bant olan%0.419'luk çok dar kesirli bant genişliğine sahiptir.Öte yandan, yarı fraktal BSF, ISM ve C bandı kablosuz uygulamalar için kalıcı frekans etkileşimlerine açık olan geniş bant kablosuz sistemlere entegre edilebilir. Ölçülen frekans tepkileri, simülasyonlar ile iyi uyum içindedir. Her filtre,

en yeni kablosuz uygulamaların ilginç özelliklerini belirten küçüklük özelliklerinin yanı sıra tatmin edici S_{11} ve S_{21} yanıtları sunar. Her tasarlanmış filtre için simüle edilen ve ölçülen frekans tepkileri, kabul edilebilir tutarsızlık ile çok iyi bir uyum içindedir.

Anahtar kelimeler: Yarı fraktal geometri, mikroserit filtreler, filtre küçüklük, dar frekans yanıt

CHAPTER ONE

INTRODUCTION

1.1 Background

The expansion of signal processing and hardware mechanisms is essential to sustain the swiftly development of the latest and complicated wireless services. Particularly, contemporary microwave architectures should satisfy progressively rigorous requirements regarding their performances, compactness and easy integration with other devices or systems [1] For this objective, microstrip band pass filter and band stop filter are electromagnetic elements which are situated at the terminal and beginning of transmitter and receiver respectively for microwave communication system. These devices represent two port networks that are important to provide signal transmission and rejection within specific bands according to wireless system requirements [2]. The elemental part of these devices is called resonator. The topology of resonators is divided into planar resonators and non-planar resonators. The planar resonators are regularly constructed using the microstrip technology. Microstrip resonators are extremely planar resonators and have huge benefits to diminish the filter size. Meandering the microstrip resonator is the most adopted methods to miniaturize the microstrip filter. For instance, the size of open loop meandered microstrip line resonator is less than $\lambda_{g0}/8$ by $\lambda_{g0}/8$, where λ_{g0} is the guided wavelength at resonant frequency [3]. But, the microstrip line must have too narrow line if more smallness using meandering is intended. This case will decrease the quality factor of the resonator as the line turns out to be narrower. This problem is fixed by High Temperature Superconducting (HTS) materials, but the cooling requirements lessen the compactness gain. In contrast, non-planar resonators have moderately better quality factor as compared with planar resonators, but they

are larger in size as in waveguide cavity filters. These non-planar filters can be utilized in wireless systems when the frequency responses of these devices are more essential than filter size as in the applications of ground cellular stations and satellite transponders [4].

1.2 Analog Filter Response Types

The applicable microstrip filter responses are categorized into of Chebychev, Cauer (elliptic) and quasi elliptic. Table 1reviews the formulas of these three cases and Figure 1.depicts their typical frequency responses [5].

Table 1: Polynomials for filter response [5].

Response type	$F_N(\Omega)$
Chebysher	$cos\|N\,cos^{-1}(\Omega)\|\,\|\Omega\|\leq1$ $cos\|N\,cosh^{-1}(\Omega)\|\,\|\Omega\|\geq1$ where Ω is normalized angular frequency
Quasi elliptic	$cosh\left\|(N-2)\,cosh^{-1}(\Omega)+cosh(\dfrac{\Omega_a\Omega-1}{\Omega_a-\Omega})+cosh^{-1}(\dfrac{\Omega_a\Omega+1}{\Omega_a+\Omega})\right\|$ Where $\Omega=\pm\Omega_a(\Omega_a>1)$ are the frequency locations of a pair of transmission zeros
Cauer elliptic	$M\dfrac{\prod_{i=1}^{n/2}(\Omega_i{}^2-\Omega^2)}{\prod_{i=1}^{n/2}(\frac{\Omega_s{}^2}{\Omega_i{}^2}-\Omega^2)}\,for\,N\,even$ $N\dfrac{\Omega\,\prod_{i=1}^{(n-1)/2}(\Omega_i{}^2-\Omega^2)}{\prod_{i=1}^{(n-1)/2}(\frac{\Omega_s{}^2}{\Omega_i{}^2}-\Omega^2)}\,for\,N\,odd\,and\geq3$ where $0<\Omega_i<1$ and $\Omega_s>1$ represent some critical frequencies
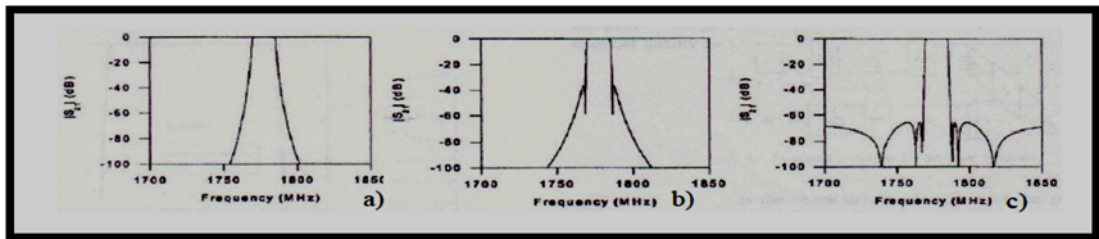
Figure 1: a) Chebychev, b) quasi elliptic and c) elliptic responses.

1.3 Types of Filters

Filters are classified according to the category of filtering role that they act upon. They can be employed in all frequency ranges and are divided into four majortypes [1-4]:

1. Lowpass filter (LPF) that conveys the entire signals from zero to $\omega_c$cut-off frequency and weakens the entire signals with frequencies aboveω_c.

2. Highpass filter (HPF) that transmits the entire signals with frequencies beyondω_c and declines signal underω_c.

3. Bandpass filter (BPF) that transmits signal within $\omega_1$to $\omega_2$frequency range and declines all frequencies out of this range.

4. Lastly, vice versa is the bandstop filter (BSF).

Figure 2 shows the frequency responses of the four filter categories.
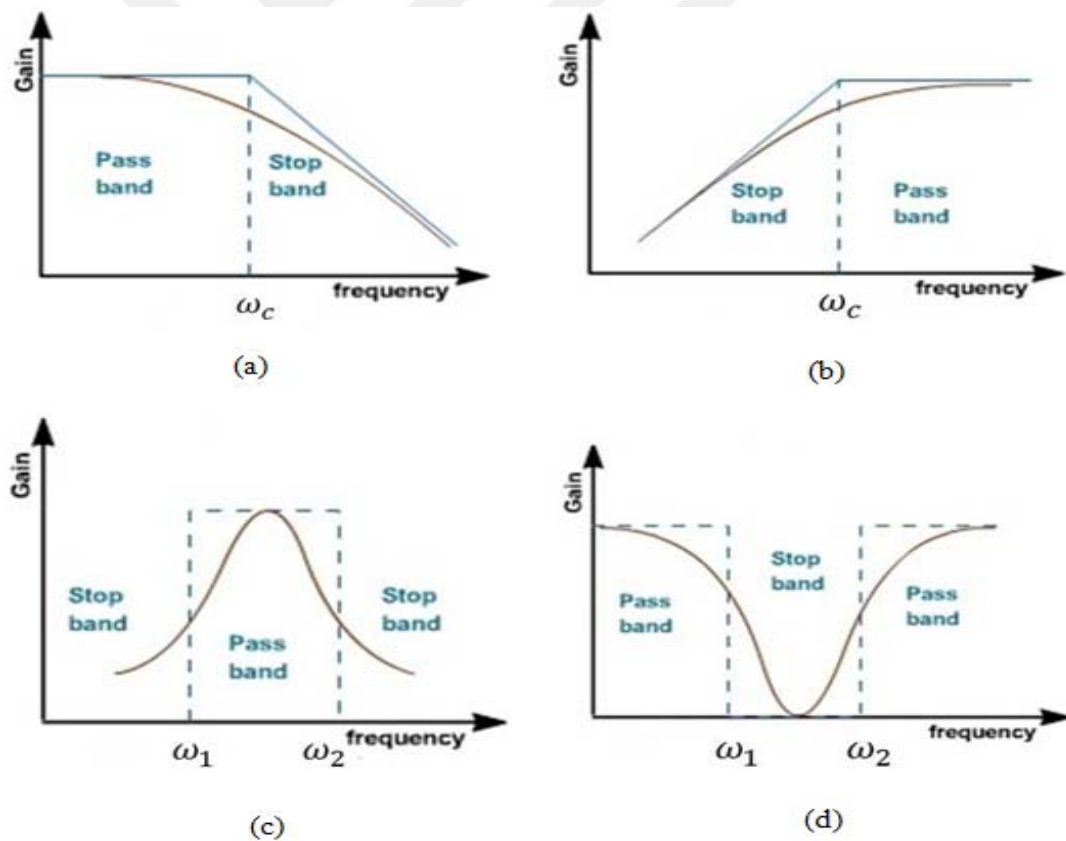
Figure 2: Frequency responses of: (a) Lowpass filter (b) Highpass filter (c) Bandpass filler, and (d) Bandstop filler.

1.4 The Main Goals of This Thesis

In this thesis, condensed microstrip filters based on dual mode resonator are designed as single and multi band stop devices. They use quasi fractal resonator as slotted patch EM elements. Theoretically, very narrow microstrip band pass filter that has fractional bandwidth less than 1 %is very rare, but in HTS filters is possible. However, HTS filters require efficient coolers to decrease the resultant heat due to narrow strips of HTS topology. This, of course, decreases the compactness benefit of this type of filters. This study is aimed to design microstrip band pass filter with very narrow fractional bandwidth that is very purposeful in wireless systems in excluding interfering signals in adjacent bands and increases hugely the quality factor of designed filter. Also, multi band bandstop filter with multi narrow band peaks is modeled to be useful for wireless system applications that require wide band responses with narrow reject band separations as in similar bandstop filter applications.

1.5 Thesis Layout

This thesis is organized as follows:

1. Chapter 1 represents the background of compact microstrip filters and the corresponding reported works in the literature.
2. Chapter 2 stands for the area of fractal terminology and reported fractal microstrip filters in the literature.
3. Chapter 3 shows the elemental theories of filters and their applications.
4. Chapter 4 includes modelling and simulation results of microstripfilters employing quasi fractal geometry.
5. Chapter 5 represents the end notes for obtained results in this study and the commendations for future work.

CHAPTER TWO

LITERATURE REVIEW

2.1 Introduction

There has been a great deal of interest regarding fractal in the literature. Microstrip filters are RF/ Microwave devices are examples that use fractals in their design and optimization. This chapter concentrates on the basics of fractals as well as state of art concerning microstrip filters using various types of fractal geometries with different intended filter responses.

2.2 Fractal Geometries

Fractals had been primarily characterized by Benoit Mandelbrot in 1975 as a technique of categorizing shapes or curves that their dimensions are not complete numbers [5]. They means split or rough fragments which has fundamental self-similarity in their geometrical structure. They are easily employed to form composite natural objects as in clouds, galaxies, mountain, leaves, trees and well-known mathematical geometries. Figure 3 shows a number of instances the fractal structures.
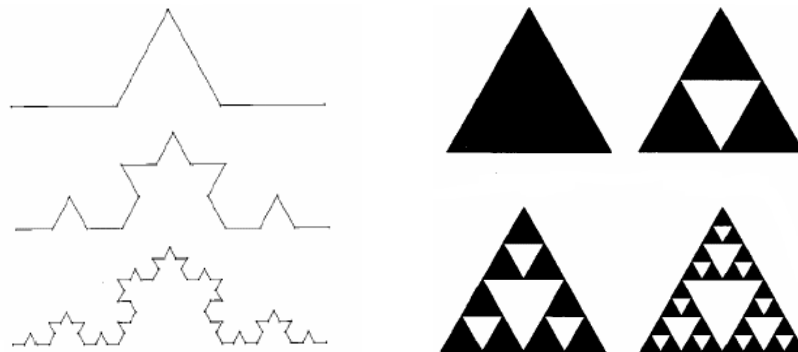
Figure 3: Examples of fractal configurations.

Therefore, fractals are things that has hierarchical topology which is self-analogous, and replicates itself more several levels [6-7]. Scientifically, drawn fractals broaden the characteristics of self-similarity downwards to small or equal to large scales arbitrarily. The factual fractals, however, comprisel east and biggest scales. These representr elevant objective representations for multiplicity of natural configurations and phenomena. An additional line of adopting fractals, that demonstrated even more productive, is a production of self-similar objects for industrial intentions as in fractal antennas [6] and filters [5, 8-17].

The swift growth of military and marketable applications has motivated new requirements of analog filters in terms of low profile, dual-band/multiband, compactness. One of the smart solutions for all these demands is the use of fractal geometry.

The fractal idiom is initiated from the Latin word "fractus," which stands for split or split parts. Benoit Mandelbrot is a mathematician who firstly defined the fractal and explained all its curves, iterations and length specifications. Fractals are constructed using a particular formula with different curve orders which are called Iterated Function Systems (IFS). They are created from the sum of duplicates of itself; each copy has smaller duplicate from the preceding orders [7].

2.3 The Literature Survey

Along with the initial uses of fractals in the filter designs is that of Yordanov*et. al*, [8]. They had designed and fabricated fractal filter. Their study is rooted in their investigation of Cantor fractal geometry. Microstrip fractal filters, subsequently, had been investigated widely in the literature using various fractal geometries such as Hilbert, Minkowski, Koch, Peano and Moore curves. These fractals are productively utilized in the design of compacted single band and dual/ multi band microstrip filters for various communication applications [9-17].

Hilbert and Minkowiski fractal geometries had been used to model and fabricate very compact HTS filters as reported in [9]. The designed filters are in diverse fractal iteration levels for different wireless applications including ISM band systems. Also, a number of 4th order topolgies, with Chebychev and quasi elliptic responses, had been manufactured.

Minkowski-like prefractal resonators are used to design microstrip bandpass filter as presented in [10] for ISM band applications. These filters uses dual mode fractal resonators as 2nd order EM component in single structure with orthogonal I/O feeders and perturbation element.

Microstrip bandpass filters using Hilbert fractal resonators with coupling stubs are designed for wireless appliance operating 2.4 GHz [11]. These filter have narrow band frequency responses with dual transmission zeros as rejection band levels. The fractal resonators are based on 2nd and 3rd iteration levels.

A study on a dual mode BPFs based on Koch -like prefractal fractal geometries with multiple iteration structures for ISM band applications at 2.4 Ghz has been presented in [12]. Koch resonators for these BPFs have been used with comer cross slotted perturbation and cut perturbation techniques. Frequency responses for these filters explain that the designed BPFs have quasi elliptic and chebyshev performance curves. A perceptible size reduction is noticed as the iteration order increases at the same frequency and using the same substrate material.

Peano fractal resonators had been adopted to design microstrip filters as single and dual mode circuits [13,14,15]. A compact microstrip bandpass filter has been presented in [13] as four pole filter. It has four capacitive eely coupled using 2nd iteration level of Peano fractal strips. Peano fractal microstrip bandpass filter with second harmonic suppression has been reported in [14]. Two single-mode capacitively coupled resonators comprise the filter configuration. Dual-mode resonator based on Peano fractal geometry had been employed to simulate a condensed microstrip bandpass filter with a quasi-elliptic frequency response at 2.45 GHz [15]. This filter has been constructed by using four parts each with a constitution of 2nd iteration iteration level of Peano geometry.

Moore fractal BPFs as 2nd order configurations had been designed in [16] for ISM band wireless system. These filters employ two edge coupled resonators based on 2nd and 3rd iteration level of Moore fractal geometries. Both filters have very good electrical specification and they have superior responses than Hilbert fractal BPFs at same designed frequency and substrate specification as well as their noticeable miniaturization and 2nd harmonic suppression.

New microstrip BPF and BSF based on Hilbert fractal geometry has been presented in [17].The designed BPF uses dual edge coupled Hilbert resonators of 2nd

iteration level and it has wide band frequency response designed at 2 and 2.2 resonant frequencies. On the other hand, BSF has been designed using dual directly coupled Hilbert resonators of the same iteration level and substrate specifications at 2.37 GHz mid-band frequency. This BSF filter has narrow rejection bandwidth which can be used in broadband wireless schemes which are susceptible to permanent frequency interferences.

New dual mode microstrip BPF has been designed around 2 GHz as stated in [18]. It uses slotted patch resonator based on customized Cantor fractal geometry. The output S11 and S21 frequency responses are interesting and parametric investigation about its perturbation length in terms of electrical specifications has been achieved in this study.

There are some constraints of microwave fractal devices including antennas and filters in terms of electrical specification [9]. Nevertheless, these constraints can be fixed by reformation techniques as in fractal reconfiguration [19-21] and like pre-fractal geometries [10, 12, 22-23]. All of them are called semi or quasi-fractals [19], that can be applied to filter design, but not a precisely fractal geometry with unlimited scale. Thus, a quasi- fractal with numerous iterations can be adopted for an exacting frequency band. Each is related to a definite scale of the fractal.

CHAPTER THREE

THEORETICAL BACKGROUND OF MICROSTRIP FILTERS

3.1 Introduction

Microstrip filters have significant applications in a lot of RF and microwave schemes. Superior performance, compact, economical and lighter weight filters are progressively integrated in different microwave circuits and organisms, since they are vital with the speedy expansion of wireless telecommunication systems.

This chapter explains the theoretical frame work of filters. Major concentration isdevoted to present the concepts of transmission line, microstrip definition, elemental filter prototyping, coupling and external quality.

3.2 Transmission Line

Transmission lines structures are specialize on transmitting electromagnetic waves at RF i.e. between 300 kHz and 300 GHz [2]. There are many types of transmission lines with different characteristics and geometries [4]. Each type has advantages and disadvantages depending on the particular application. The transmission lines of the microstrip type will be used in this work. Microstrip line is regularly employed with Microwave Integrated Circuit (MIC) transmission line or Monolithic Microwave Integrated Circuit (MMIC) transmission line. It has many advantages such as; small size, low-priced, absence of critical matching and cutoff frequency, photolithographic technique (for circuit manufacture), high-quality reproducibility, and compatibility with monolithic circuit [4].

3.3 Microstrip Line Structure

The universal structure of a microstrip is shown in Figure 4. A metal strip with a thickness *(t)* and width *(W)* is on the top of a dielectric substrate that comprises a height*(h)* and dielectric constant *(εᵣ)*, and on the bottom of substrate is a ground (conducting) plane [1].
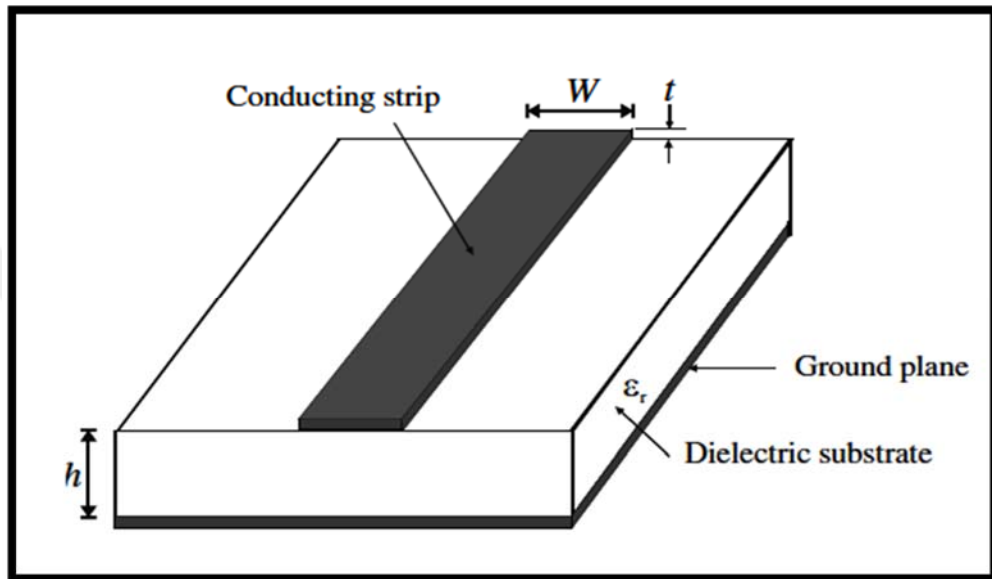

Figure 4: Microstripstructure [1].

The basic transmission line must be homogeneously distributed in terms of lumped elements as R, G, L and C which correspond to resistance, shunting conductance, inductance and capacitance, respectively, per unit length as shown in Figure 5 [1, 2, 4].
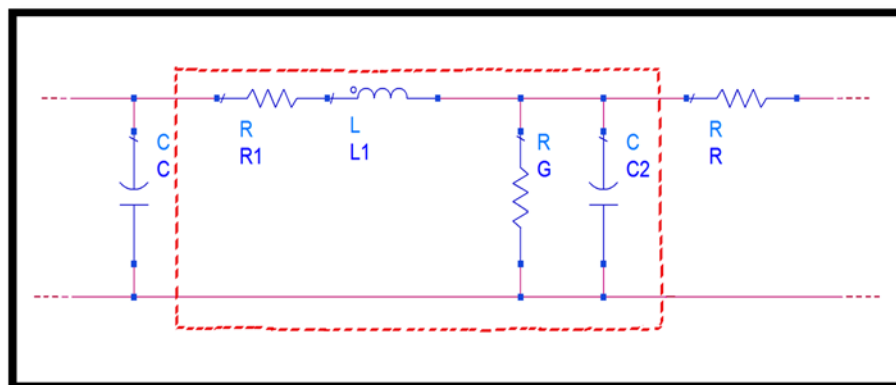

Figure 5: C, L, R and G are elements of the transmission line.

3.4 Microstrip Components

In a microstrip filter design, microstrip components may contain lumped element (capacitors and inductors), quasi-lumped elements (stubs and short line parts) and resonators. The resonators are the distributed elements in most cases use such as half-wave length and quarter-wave length line resonators. The types of filters are necessary to choice of component, the quality factors or acceptable losses, the fabrication techniques, the operating frequency and the power handling [1].

3.5 Microstrip Resonators

A microstrip resonator is EM component which can be classified into lumped, quasi-lumped, patch and distributed-line resonators.

Quasi-lumped element and lumped element resonators can be realized using lumped or quasi-lumped capacitors and inductors. At upper resonant frequencies, these elements are no longer practical. This sortof resonators haspotential immediate conversionto an equivalent circuit including inductors and capacitors into a microstrip structure [1].

The allocated magnetic and electric fields of resonators over the entire resonant constitution are known as distributed resonators. Microstrip line section is a simplest distributed microstrip resonator [2,4].

The distributed line resonator termed as a quarter wavelength $\lambda_{g0}/4$ resonator (where λ_{g0} is the guided wavelength at the elemental resonant frequencyf_0). This resonator can be short-circuited stub (equivalent to parallel LC) or open-circuit stub (equivalent to series LC resonator). Another type used in microstrip filters implementation is $\lambda_{g0}/2$ resonator. The major disadvantages of the distributed line resonators are conductor loss, dielectric dissipation loss and radiation losses which are subjected to the applied line lengths [4].

Another kind of distributed line resonator which is the ring resonator. It is an uncomplicated transmission line where the resonator is induced at a definite range of frequencies. Based on the electrical length at resonant frequency, a pattern of standing wave can be generated in the region of the circular path of the resonator [4].

The patch resonators have been highly desired for microstrip filter designs in view of the fact that they have less conductor losses and advanced power treatment

capability than typical microstrip line resonators. Patch resonator may take different forms depending on the applications, such as Triangular or Circular [4, 18].Figure 6 shows these types.
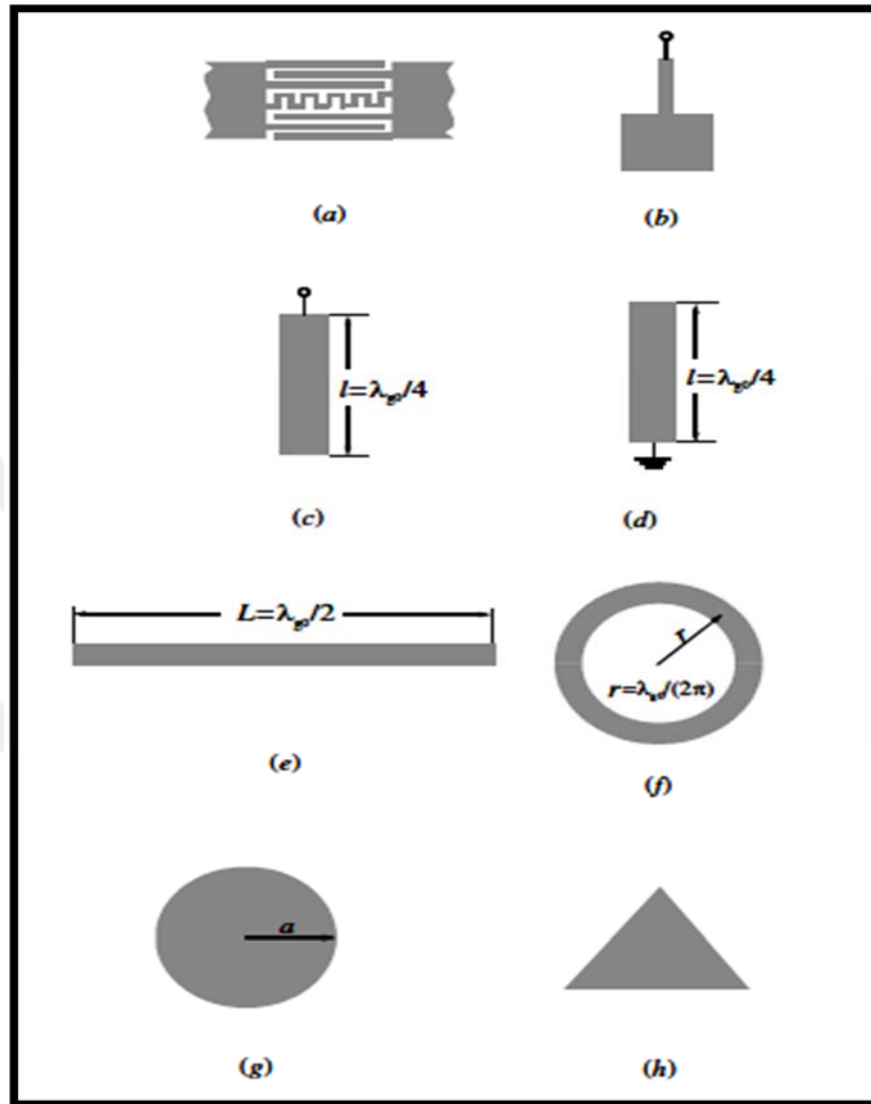
Figure 6: Some models of microstrip resonators: (*a*) lumped element resonator, (*b*) quasi-lumped element resonator, (*c*) $\lambda_g/4$-line resonator (shunt series resonance), (*d*) $\lambda_g/4$-line resonator (shunt parallel resonance), (*e*) $\lambda_g/2$-line resonator, (*f*) ring resonator; (*g*) circular patch resonator, (*h*) triangular patch resonator [1].

3.6 Transmission Line Resonator and SIR [1,4]

Coaxial, strip and microstrip line resonators are the common examples of transmission line resonators that supports Transverse Electromagnetic Mode (TEM) or quasi-TEM modes.

Transmission line resonators stand for Uniform Impedance Resonator (UIR). A high permittivity, lower loss tangent, and temperature stabilization for the Dielectric substrate material are the generic requirement for UIR. Because of easy and simple structure in the design, the UIRs are vastly used in designs.

In feasible design, while these resonators have uncomplicated structure, other electrical downsides contain spurious responses at integer manifolds of the essential frequency. These problems can be fixed by using capacitor loads at open-terminals of the resonator. It is a popular practice in the very high frequency band regions. Therefore, the dimension of resonator is shorter while the spurious resonant frequencies are accordingly reallocated from multiple integers of the essential frequency.

The structure difference of $\lambda_{g0}/2$ resonator is explained in Figure 7. The capacitor loaded UIR in this outline has an electrical length of $2\theta_1$ and characteristic impedance of Z_1. When ω_0 (radian resonant frequency) of this resonator agrees to half-wavelength UIR depicted in (a), the loading capacitance can be determined as:

$C = Y_1 \tan \theta_2/\omega_0 ...(3.1)$

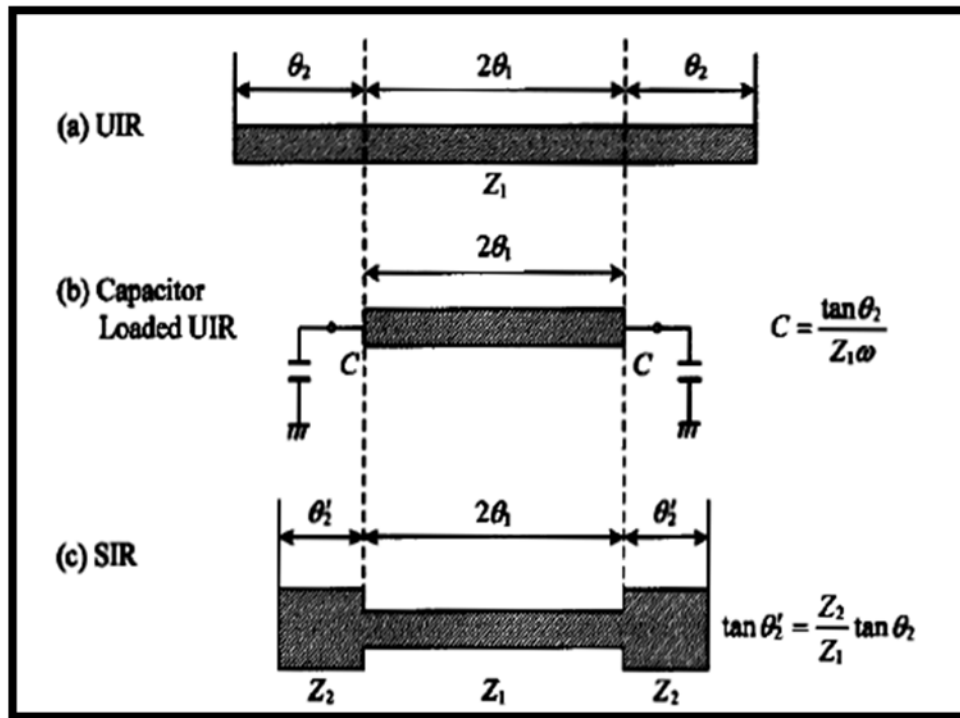Where $\theta_2 = \pi/4 - \theta_1, Y_1 = 1/Z_1 ...(3.2)$

Figure 7: Structure variation a half-wavelength resonator. (a) UIR. (b) Capacitor loaded UIR. (c) SIR [2].

From Figure 7 (a), both transmission line components with electrical lengths of θ_2 are replaced with capacitors as in (b). The capacitor loaded UIR has the abilities to suppress spurious response and it has relatively small size.

However, in the frequency around 1 GHz, it is not frequently simple to stratify the capacitor loaded UIR, because loss in the lumped element capacitor rises noticeably as resonant frequency increases. Thus, frequency modification is needed in this case.

The loaded capacitance can be altered by an open-circuit transmission line. Besides, it is not compulsory for all time to realize the characteristic impedance of transmission line atZ_1. Figure 7(c) shows the characteristic impedance generated at$Z_2 = (1/Y_2)$. If $Y_2 \tan \theta_2^{'} = Y_1 \tan \theta_2$, All components will be resonant at identical frequency. Accordingly, if Z_2 is less thanZ_1, then, $\theta_2^{'} < \theta_1$.So, the length of resonator can be short-ended. In addition, the removal of capacitor enables UIR to display more features including a small measure of resonance frequency difference and low-loss properties. So, this design overcomes on the formerly displaying weak points when it uses capacitor loaded shown in Figure 7(b).

Figure 7(c) illustrates Stepped Impedance Resonator (SIR) which has distinctly dissimilar characteristic impedances.

3.7 SIR Basic Structure [1,4]

SIR is a TEM or quasi-TEM component which has dual or more varied characteristic impedances as shown in Figure 8. This figure shows the typical examples of its structural difference in the case of the strip line arrangement, where Figure 8(a, b and c) respectively, are examples of$\lambda_g/4, \lambda_g/2$, and λ_g-type resonator. Alternative transmission-line structure other than the illustrated stripline configuration, such as coplanar and coaxial-line, are acceptable with the condition of TEM /quasi-TEM mode resonance. While the$\lambda_g/2$-type SIR shown in 8(b) employs an open-ended structure, short-circuited structures are also available.

Z_1andZ_2 are characteristic impedances of SIR components while $\theta_1$and θ_2 are electrical lengths of transmission lines involving the short-and open-circuited ends as shown in Figure 8.
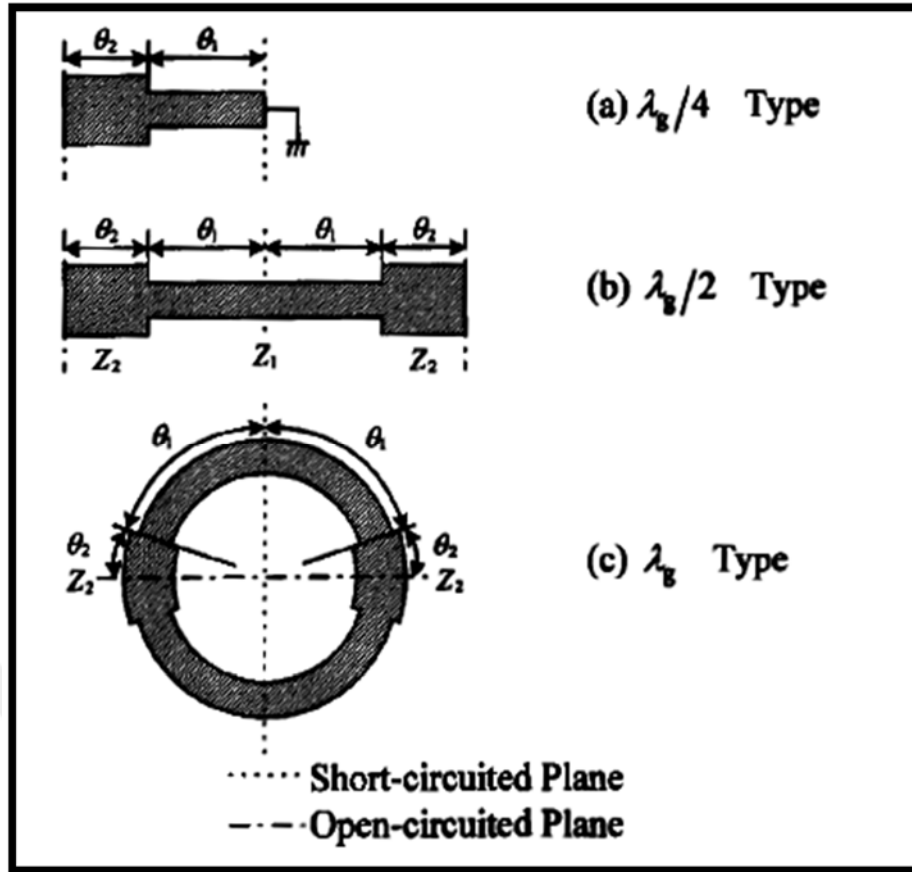
Figure 8: The SIR basic structure. (a) Quarter wavelength$(\lambda_g/4)$. (b) Half wavelength$(\lambda_g/2)$. (c) One wavelength (λ_g) [2].

The imperative parameter in characterizing the properties of the SIR is represented by R_z which is the transmission line impedances Z_2 andZ_1 ratio as follows [27]:

$R_z = Z_2/Z_1$ Impedance ratio …(3.3)

3.8 Characteristic Impedance and Effective Dielectric Constant [1]

In the quasi-TEM rough calculation, an identical dielectric material with an effective dielectric permittivity substitutes the non-identical dielectric–air media of microstrip. The Characteristic impedanceZ_0 and effective dielectric constant ε_{re} are essential to describe the transmission impedance of microstrips. For extremely skinny conductors$(i.e, thicness \rightarrow 0)$, the closed form expression which supplies a precision as follows.

For $W/h \leq 1$:

$$\varepsilon_{re} = \frac{\varepsilon_r+1}{2} + \frac{\varepsilon_r-1}{2}\left[\left(1 + 12\frac{h}{W}\right)^{-0.5} + 0.04\left(1 - \frac{W}{h}\right)^2\right] \tag{3.4}$$

$$Z_0 = \frac{60}{2\pi\sqrt{\varepsilon_{re}}} ln\left(\frac{8h}{W} + 0.25\frac{W}{h}\right) \tag{3.5}$$

For $W/h \geq 1$:

$$\varepsilon_{re} = \frac{\varepsilon_r+1}{2} + \frac{\varepsilon_r-1}{2}\left(1 + 12\frac{h}{W}\right)^{-0.5} \tag{3.6}$$

$$Z_0 = \frac{377}{\sqrt{\varepsilon_{re}}\left[\frac{W}{h}+1.393+0.677\, ln\left(\frac{W}{h}+1.444\right)\right]} \tag{3.7}$$

The width of microstrip corresponding to a known Z_0 is obtained for [28].

$$W/h \leq 2$$

$$\frac{W}{h} = \frac{8exp(A)}{exp(2A)-2} \tag{3.8}$$

Where

$$A = \frac{Z_0}{60}\left[\frac{\varepsilon_r+1}{2}\right]^{0.5} + \frac{\varepsilon_r-1}{\varepsilon_r+1}\left[0.23 + \frac{0.11}{\varepsilon_r}\right] \tag{3.9}$$

And for $W/h \geq 2$

$$\frac{W}{h} = \frac{2}{\pi}\left[(B-1) - ln(2B-1) + \frac{\varepsilon_r-1}{2\varepsilon_r}\left[ln(B-1) + 0.39 - \frac{0.61}{\varepsilon_r}\right]\right] \tag{3.10}$$

Where

$$B = \frac{377\pi}{2Z_0\sqrt{\varepsilon_r}} \tag{3.11}$$

3.9 Propagation Constant, Guided Wavelength, Electrical Length and Phase Velocity [1,2,4]

When the effective dielectric constant (ε_{re}) of a microstrip is calculated, the guided wavelength is given by:

$$\lambda_g = \frac{\lambda_0}{\sqrt{\varepsilon_{re}}} \tag{3.12}$$

Where λ_0 represents the free space wavelength while f represents the operating frequency. The guided wavelength is determined by

$$\lambda_g = \frac{300}{f(GH_z)\sqrt{\varepsilon_{re}}}mm \tag{3.13}$$

The phase velocity v_p and associated propagation constant β are computed by

$$\beta = \frac{2\pi}{\lambda_g} \tag{3.14}$$

$$v_p = \frac{\omega}{\beta} = \frac{c}{\sqrt{\varepsilon_{re}}} \tag{3.15}$$

The light speed (*c)* in free space is $3 \times 10^8 \ meter/second$.

From a certain physical length (*l),* the electrical length of the microstrip is calculated by:

$$\theta = \beta l \tag{3.16}$$

when $l = \lambda_g/2$, then$\theta = \pi$ and when$l = \lambda_g/4$, then $\theta = \pi/2$ and These called half-wavelength and quarter-wavelength microstrip lines are vital for design of microstrip filters [23].

2.10 Microstrip Losses

The loss constituents of a single microstrip line consist of conductor loss in the ground plane and strip, dielectric loss in substrate, Surface wave loss and radiation loss [4].

The losses are symbolized as a loss per unit length along the microstrip line in terms of the attenuation factor α. In dielectric substrates, the dielectric losses are on averagefewer than conductor losses. Nevertheless, dielectric losses in silicon substrates can be of the same order or larger than conductor losses [1,4].

Discontinuities of the microstrip line is producing radiation to free space. The radiation loss (housing loss) rises rapidly as the frequency rises. To avert interference and leakage, microstrip circuits are commonly protected inside a metal box. In microstrip antennas, radiation leakage has benefit in usage.

The waves that are trapped by full reflection inside the substrate is called Surface waves. They may generate undesirable radiation from the brink of substrate and pseudo coupling among elements [4].

3.11 Microstrip Filter Design

Microstrip filter realizations have many basics and theories for RF and Microwave frequency applications as follows:

3.11.1 Microstrip Lowpass Filters Design [1,2,4]

As a general rule, the design of microstrip LPF includes dual foremost steps:
1) Selection of the suitable low pass prototype. The option of the type of

response, involving the pass band ripple and number of reactive elements, will depend on the desired specifications. The element values of the filter, are typically normalize, then transformed to LC constituents for the required cut off frequency and mandatory source impedance, which is ordinary for microstrip filters 50 ohms to obtain an appropriate lumped-element filter design.

2) Find a suitable microstrip realization. It is used to get an investigation in order to approximate the lumped element filter. Several microstrip realizations, for example stepped-impedance LC ladder of low pass filters and LC ladder low pass filter employing open-circuited Stubs.

3.11.1.1 Selection of suitablelowpass prototype filters

Lowpass prototype filter is theoretically normalized with unity values of source resistance or conductance (g_0=1) as well as the cutoff angular frequency ($\Omega_c = 1$ rad/s). Dual potential structures of lowpass prototype for n-pole filter realization for Gaussian, Chebyshev as well as Butterworth responses are shown in Figure 9 [2,4].
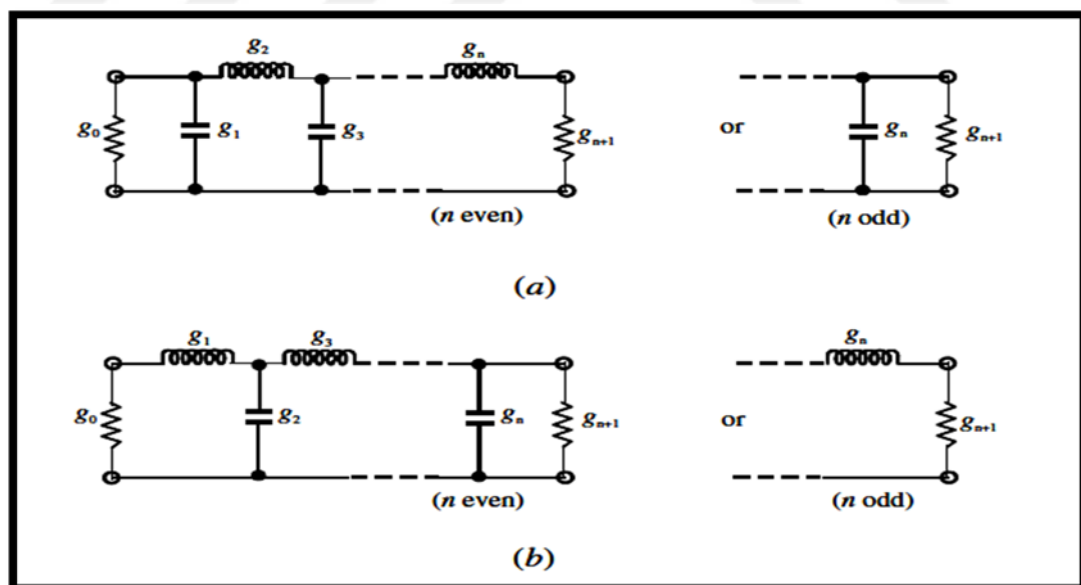

Figure 9: All-pole filters lowpass prototyping filters with (a) a ladder network (πtype) structure and (b) its dual (T type) [1].

In Figure 9, g_i for i = one to n symbolize both inductance and capacitance by using a shunt capacitor or a series inductor. So, n is the interactive element number.

If g_1 is series inductance or shunt capacitance, then g_0 is known as the source conductance or resistance. Identically, when g_n stands for the series inductance or shunt capacitance, g_{n+1} in this case turns into the conductance or resistance load. On the other hand when unless specified g magnitudes may be considered as capacitor element in farad units, inductance in henry units, conductance in mho units, and resistance in ohm units. This kind of LPF can be availed as a prototype to model numerous effective filters.

To obtain element values and frequency characteristics for realistic filters derived from the lowpass prototype, frequency and element transformations can be adopted in this case.

The frequency transformation, which is also refers to frequency mapping, is necessary to realize a frequency response, for example, Chebyshev response in the lowpass prototype from (Ω) to (ω) frequency domain in which a realistic filter response as in highpass, lowpass, bandstop and bandpass responses can be mapped from it. This transformation will have no impact on the resistive parts, but change all the reactive parts [23].

Impedance scaling is required in addition to frequency mapping to achieve the element transformation. It is used to eliminate unity normalization for g_0 value. Also, to set the filter to act for whichever magnitude of source impedance (Z_0). In this matter, it is suitable for an impedance-scaling factor definition (y_0) as [2]:

$$y_0 = \begin{cases} Z_0/g_0 & \text{for } g_0 \text{ can be resistance} \\ g_0/Y_0 & \\ & \text{for } g_0 \text{ can be conductance} \end{cases} \tag{3.17}$$

where Y_0 is the source admittance $(Y_0 = 1/Z_0)$.

Also, it has the possibility to transform from a lowpass prototype to a practicable LPF within a cutoff frequency (ω_c) and angular frequency axis (ω) by [1,4]:

$$\Omega = \left(\frac{\Omega_c}{\omega_c}\right)\omega \tag{3.18}$$

so equation of the element transformation:

$$L = \left(\frac{\Omega_c}{\omega_c}\right)y_0 g \tag{3.19}$$

$$C = \left(\frac{\Omega_c}{\omega_c}\right)\frac{g}{y_0} \tag{3.20}$$

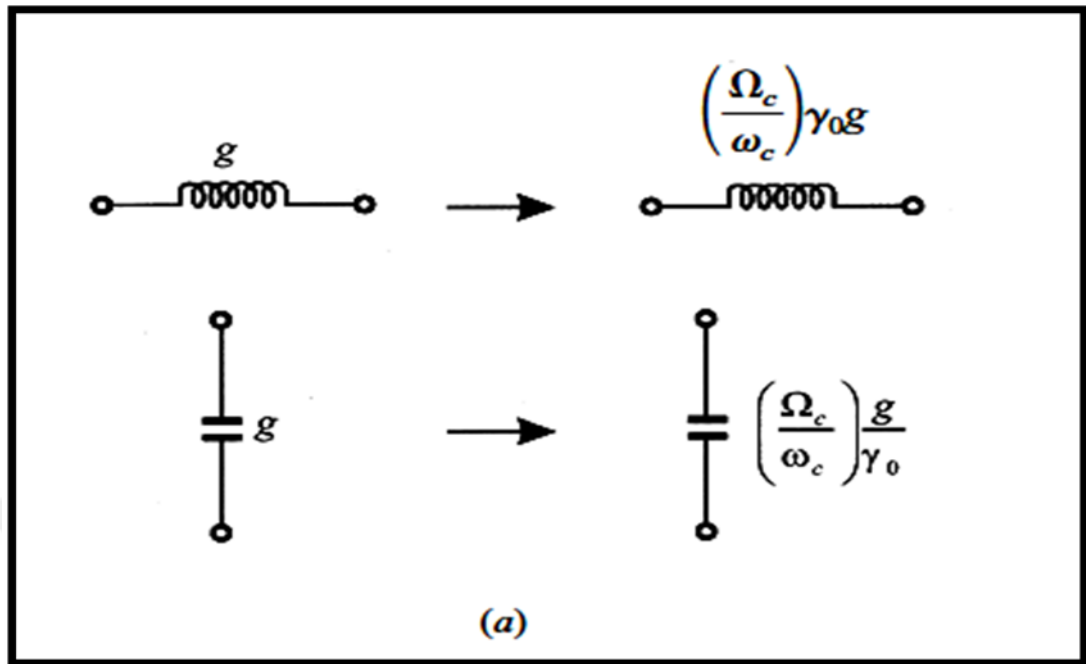Figure 10 shows these elements.

Figure 10: Lowpass prototype to lowpass transformation [1].

3.11.1.2 Find a suitable microstrip realization [1,4]

In this subsection, some of microstrip realizations will be described.

a) Stepped-impedance, LC ladder type lowpass filter:

Figure 11(a) explains common constitution of SIR low pass microstrip filters, that exploit a cascading structure of alternative low- and high impedance transmission lines. They are less than λ_g, in order to operate as semi lumped elements. The low-impedance lines represent shunt capacitors and the series inductors are represented by high-impedance lines. Consequently, the structure of this filter can be straight forwardly realized using the L-C ladder class of lowpass filters in Figure 11(b).
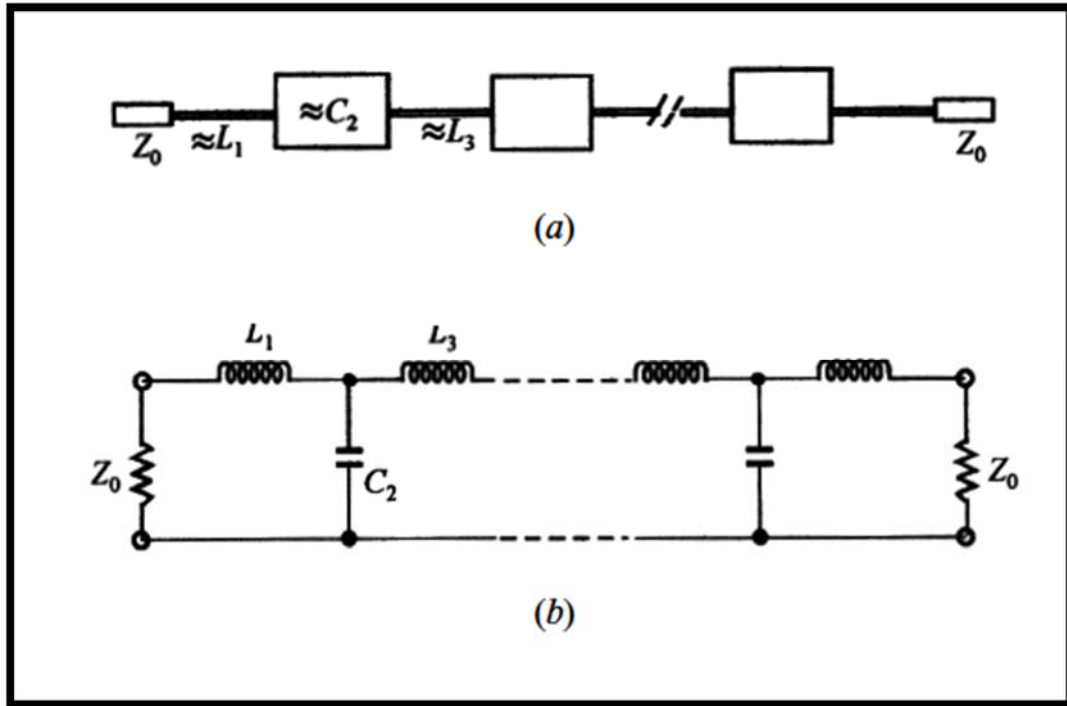
Figure 11: (*a*) Commonformation of the stepped-impedance low pass microstrip filters. (*b*) L-C ladder class of lowpass filters [1].

Several information about filter design should be given regarding the microstrip lines, since capacitance and inductance expressions rely on characteristic impedance and length of microstrip line. It will be useful to primarily specify the low-and high the characteristic impedances lines by keeping of:

1) $Z_{0C} < Z_0 < Z_{0L}$, where Z_{0L} and Z_{0C} symbolize the characteristic impedances of the high and low impedance lines, and the source impedance is Z_0, for microstrip filters is usually 50 ohms.

2) A bigger value of Z_{0L} causes a superior rough calculation of a lumped-element inductor, but Z_{0L} value shouldn't be too huge because its manufacturing is very tricky as a narrow line and that represent very confused limitation.

3) A lower Z_{0C} causesanenhancedrough calculation of a lumped-element capacitor, nevertheless the consequential line width W_C does not have totolerate which ever transverse resonance to arise at operation frequencies.

b) Open-circuited stubs for LC ladder type of lowpass filters realization [1,4]:

The stepped impedance LPF can be initiated using low impedance lines with shunt capacitors as lowpass prototype in the transmission path. Another option to realize a shunt capacitor is by employing an open-circuited stub as follows:

$$\omega C = \frac{1}{Z_0} \tan\left(\frac{2\pi}{\lambda_g} l\right) \, for \, l < \lambda_g/4 \tag{3.21}$$

The input susceptance of open-circuited stub term is represented on the right hand side while susceptance of shunt capacitor term can be observed on the left-hand side, when the physical length l and characteristic impedance Z_0 which is less than $\lambda_g/4$.

To achieve the lumped LC elements, the electrical lengths of the high-impedance lines and the open-circuited stub are firstly calculated as:

$$l_L = \frac{\lambda_{gL}}{2\pi} \sin^{-1}\left(\frac{\omega_c L}{Z_{0L}}\right) \tag{3.22}$$

$$l_C = \frac{\lambda_{gC}}{2\pi} \tan^{-1}(\omega_c C Z_{0C}) \tag{3.23}$$

The filter is offered a better stop band characteristic when using an open-circuited stub, for the reason that at limit frequency, the open-circuited stub is about $\lambda_g/4$ in order tonearly short out a transmission, andinitiate the attenuation peak.

3.11.2 Microstrip Bandpass Filters Design

The bandpass filter (BPF) design also using the same two Steps of the lowpass filters design but in different equation so in the step one, the equations of lumped values of the BPF after limitation the prototype values to the filter, frequency and impedance scaling given by:

The series LC resonator elements in the BPF are

$$L_s = \left(\frac{\Omega_c}{FBW\omega_0}\right) y_0 g \tag{3.24}$$

$$C_s = \left(\frac{FBW}{\omega_0\Omega_c}\right) \frac{1}{y_0 g} \tag{3.25}$$

Where FBW stands for the fractional bandwidth of BPF.

Likewise, the parallelLCresonator elements in the BPF are

$$C_p = \left(\frac{\Omega_c}{FBW\omega_0}\right) \frac{g}{y_0} \tag{3.26}$$

$$L_p = \left(\frac{FBW}{\omega_0\Omega_c}\right) \frac{y_0}{g} \tag{3.27}$$

The transformations of these elements are shown in Figure 12. For this case, using similar lowpass prototype and it is distinguished that $\omega_0 L_s = 1/(\omega_0 C_s)$ and $\omega_0 L_p = 1/(\omega_0 C_p)$.
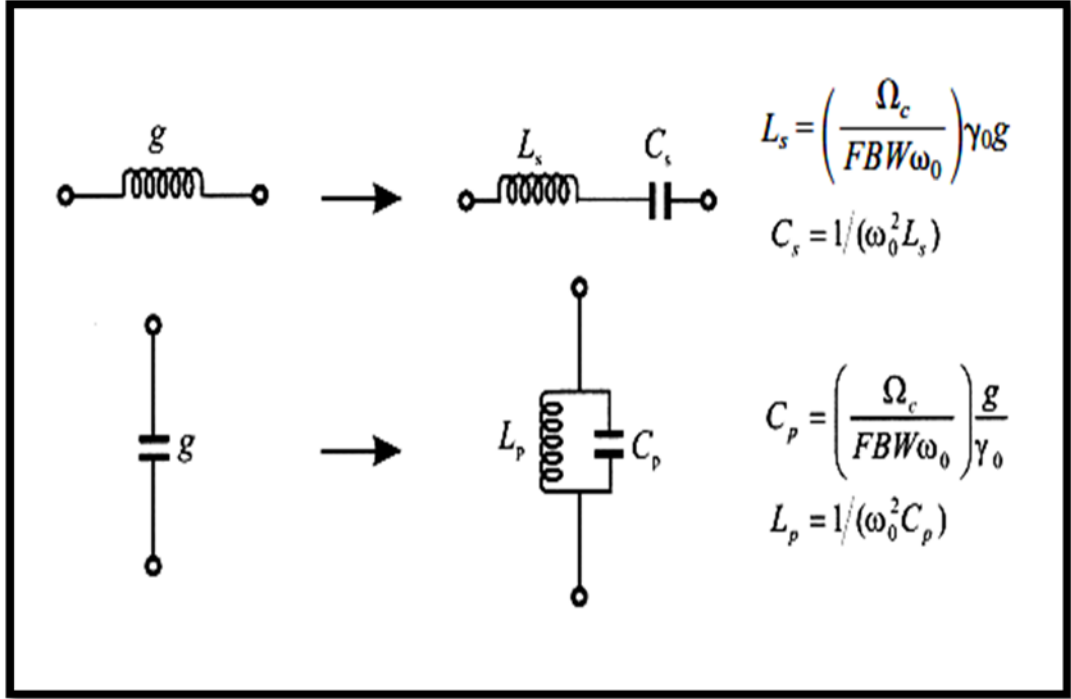
Figure 12: Basic element transformation from lowpass prototype to bandpass structure [1].

The next step to design BPF using parallel-coupled type, the design equations of filter are given by:

$$\frac{J_{01}}{Y_0} = \sqrt{\frac{\pi}{2}\frac{FBW}{g_0 g_1}} \tag{3.28}$$

$$\frac{J_{j,j+1}}{Y_0} = \frac{\pi FBW}{2}\frac{1}{\sqrt{g_j g_{j+1}}} \quad j=1 \text{ to } n-1 \tag{3.29}$$

$$\frac{J_{n,n+1}}{Y_0} = \sqrt{\frac{\pi}{2}\frac{FBW}{g_n g_{n+1}}} \tag{3.30}$$

Where g_0, g_1...g_n are the element of a ladder-type lowpass prototype with a normalized cutoff $\Omega_c = 1$, and Y_0 stands for the characteristic admittance of the terminating lines and $J_{j,j+1}$ represent the characteristic admittances of *J*-inverters.

On the way to achieve the *J*-inverters as above, odd and even mode characteristic impedances must be evaluated for the joined microstrip line resonators by:

$$(Z_{0e})_{j,j+1} = \frac{1}{Y_0}\left[1 + \frac{J_{j,j+1}}{Y_0} + \left(\frac{J_{j,j+1}}{Y_0}\right)^2\right] \quad j= 0 \text{ to } n \tag{3.31}$$

$$(Z_{0o})_{j,j+1} = \frac{1}{Y_0}\left[1 - \frac{J_{j,j+1}}{Y_0} + \left(\frac{J_{j,j+1}}{Y_0}\right)^2\right] \quad j= 0 \text{ to } n \tag{3.32}$$

23

3.12 Coupled Line [1,4]

When assuming a TEM form of propagation, then the electrical characteristics of the coupled lines is fully evaluated from the effective capacitances flanked by the line and the velocity of propagation on the line. The coupled microstrip line is shown in Figure 13.
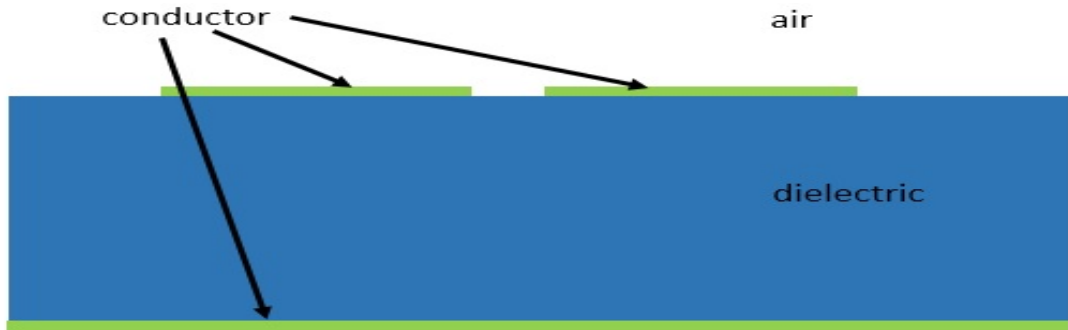

Figure 13: The coupled microstrip structure. (redrawn).

2.13 Coupling between Resonators [1,4, 9]

Coupled resonator filters are widely reported in the many research articles for various applications. In fact, there is a common procedure for scheming these filters that can be adopted to all types of resonator at any rate of its topological constitution. In the SIR component, the circuit uses dual pairs of coupled line as described in Figure 14 as compared with UIR.

From the first section of coupled lines in Figure 14, it has a short circuited part and can be evaluated using odd and even mode impedance Z_{0o1}, Z_{0e1} and coupled line lengthθ_1. In this part, the controlling is inductive coupling because a big current flow close to the short circuited point. Coupled- lines 2 contains the open end of the resonator, it uses physical parameters symbolized as Z_{0o2}, Z_{0e2} andθ_2. In this part, the controlling is capacitive coupling because a big voltage closes to the open end. The geometric means for odd- and even mode impedance is given to the Z_2 and Z_1 for single transmission line SIR by equations as follows:

$$Z_1 = \sqrt{Z_{0o1} . Z_{0e1}} \tag{3.33}$$

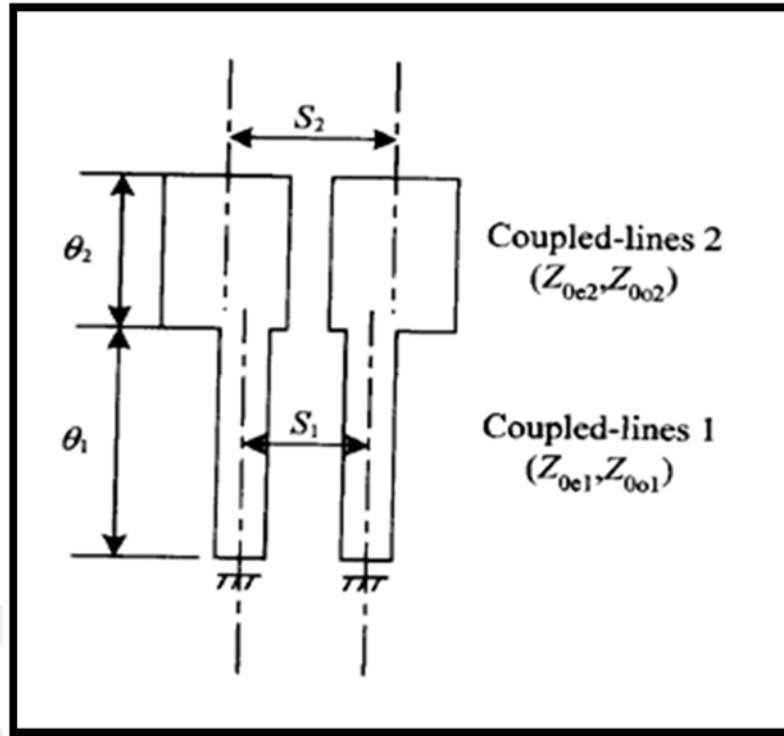$$Z_2 = \sqrt{Z_{0o2} . Z_{0e2}} \tag{3.34}$$

Figure 14: The coupling line structure of SIR. [9].

3.14 Coupling Factor and External Quality Factor

Specifically, the measurements of a Chebychev filter are corresponding to the poles number or filter order N, the mid-band frequency f_o, the in-band ripple ϵ, and bandwidth BW. By these parameters, the coupling coefficients between resonators and Q_{ext} are calculated by [1, 9]:

$$k_{i,i+1} = \frac{BW}{\sqrt{g_i \cdot g_{i+1}}} \text{ for } i = 1 \text{ to } (N-1) \quad (3.21)$$

$$Q_{ex1} = \frac{g_0 \cdot g_1}{BW} \quad (3.22)$$

$$Q_{exN} = \frac{g_N \cdot g_{N+1}}{BW} \quad (3.23)$$

g_i stands for the general coefficients of the LPF prototype. These coefficients are relied on N and ϵ and they are determined through methodical rules [1,4,9]. A number of coefficients for the specified ϵ magnitudes have been clarified in Table (3.2). For quasi elliptic responses, the zero locations regarding the band edges must be included as well in the specifications and this approach is in theory more complicated since an accurate methodical formulation is not available yet.

25

On the other hand, Many reported expressions and tables are existing for the low-pass coefficients of several fundamental quasi elliptic filter topologies with various filter orders. The modelling of a microstrip filters can be inspected efficient recent EM simulators which by inputting the substrate features and constructing all the geometric topology of projected filters including the resonator dimensions, the gapamid them and the presumed feeder configurations.

Table 2: Chebychev low pass prototype filter parameters [9].

Value of N	g_1	g_2	g_3	g_4	g_5	g_6	g_7	g_8	g_9	g_{10}	g_{11}
					0.01-dB Ripple						
1	0.0960	1.0000									
2	0.4488	0.4077	1.1007								
3	0.6291	0.9702	0.6291	1.0000							
4	0.7128	1.2003	1.3212	0.5476	1.1007						
5	0.7563	1.3049	1.5773	1.3049	0.7563	1.0000					
6	0.7813	1.3600	1.6896	1.5350	1.4970	0.7098	1.1007				
7	0.7969	1.3924	1.7481	1.6331	1.7481	1.3924	0.7969	1.0000			
8	0.8072	1.4130	1.7824	1.6833	1.8529	1.6193	1.5554	0.7333	1.1007		
9	0.8144	1.4270	1.8043	1.7125	1.9057	1.7125	1.8043	1.4270	0.8144	1.0000	
10	0.8196	1.4369	1.8192	1.7311	1.9362	1.7590	1.9055	1.6527	1.5817	0.7446	1.1007
					0.1-dB Ripple						
1	0.3052	1.0000									
2	0.8430	0.6220	1.3554								
3	1.0315	1.1474	1.0315	1.0000							
4	1.1088	1.3061	1.7703	0.8180	1.3554						
5	1.1468	1.3712	1.9750	1.3712	1.1468	1.0000					
6	1.1681	1.4039	2.0562	1.5170	1.9029	0.8618	1.3554				
7	1.1811	1.4228	2.0966	1.5733	2.0966	1.4228	1.1811	1.0000			
8	1.1897	1.4346	2.1199	1.6010	2.1699	1.5640	1.9444	0.8778	1.3554		
9	1.1956	1.4425	2.1345	1.6167	2.2053	1.6167	2.1345	1.4425	1.1956	1.0000	
10	1.1999	1.4481	2.1444	1.6265	2.2253	1.6418	2.2046	1.5821	1.9628	0.8853	1.3554

The majority of the EM simulators use orarerooted from the method of moment as an evaluation procedure. They determine the frequency responses of filter by primary partitioning the resonators in diminutivemesh, fewer or further fixed in accordance with the considered precision, and subsequently resolving linear integral equations. Then, the dimensions and topology of the resonators, for a prearranged coupling, the coefficient $k_{i,j}$ in terms of coupling space (d) can be evaluated by the transmission response analysis of two resonators, as they are slightly coupled to the exterior feed lines. Definitely, by this essential requirement, it is feasible to demonstrate that the equivalent $|S_{21}|$ hasdualtypical peaks at frequency f_1 and f_2 as in Figure 15, symmetrically around f_0. The coupling coefficient can be determined by [1, 9]:

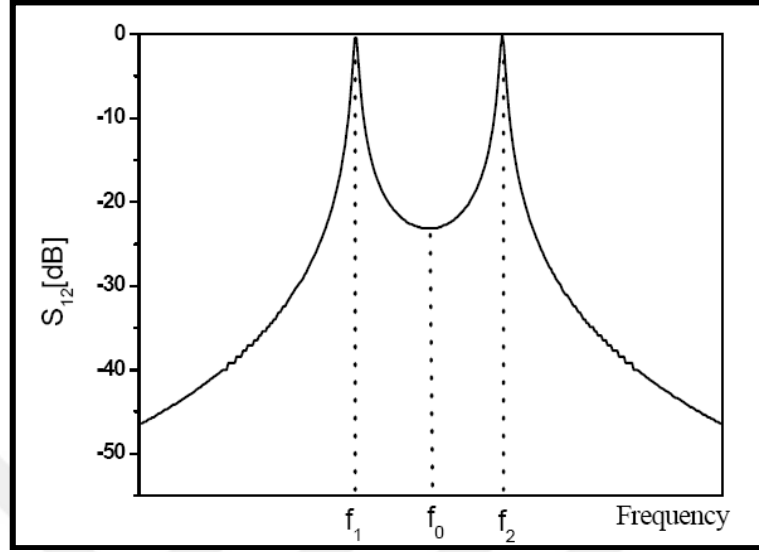$$K_{12} = \frac{2(f_2 - f_1)}{(f_2 + f_1)}$$ (3.24)

Figure 15: In general transmission response of two coupled resonators [1].

By the same procedure, Q_{ext} can be determined. The resonator can be singly loaded resonator by just coupling to input port or to be doubly loaded resonator if it connected to both input/output ports as illustrated in Figure 16 [1]. O on the other hand, Q_{ext} can be determined from the phase response S_{11} as follows:

$$Q_{ext} = \frac{f_{(0^o)}}{f_{(-90^o)} - f_{(+90^o)}}$$ (3.25)

In the last case, the resonator has been employed as first order filter and Q_{ext} is extracted from -3dB bandwidth transmission peak by:

$$Q_{ext} = \frac{2f_o}{BW_{3dB}}$$ (3.26)
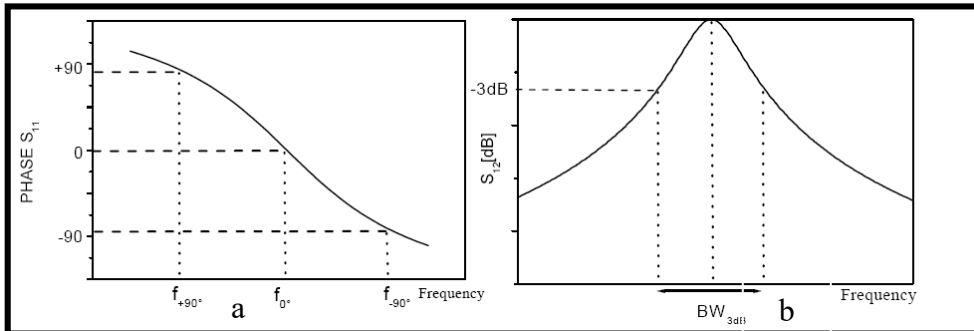
Figure 16: Q_{ext} computation for (a) Singly and (b) Doubly loaded resonator [1].

CHAPTER FOUR

DESIGN AND SIMULATION RESULTS

4.1 Introduction

In this chapter, dual mode microstrip filters are introduced for the prerequisites of contemporary wireless communication systems. The planned filters are assembled from quasi fractal resonator. The filters have condensed size and very small band responses that are the requirements of portable and telecommunication wireless schemes. The responses of filters are analyzed using Advance Wave research (AWR$_{12}$) and EM Sonnet simulators.

The procedural steps for designing microstrip filters are comprehensive as in Figure17 according to adopted circuit design.

The designed filters are run within given frequency range and prearranged step frequency. Fitting boundary conditions are dedicated by these EM simulators, in that case mesh partitioning for filter structures has been performed to acquire ending superior mesh. In mesh partitioning, it is eminent that smaller mesh is going to provide further divisions and accurate solution for intended filter response. All the same, smaller mesh is going to involve extra time for model processing. For that reason, it is compulsory to choose the good set of scales involving processing time and a sufficient accuracy level.

The fixed solver of EM simulation tools employs a linear solver procedure for model processing. The implementation of quasi fractal filters is run by Core i5 CPU computer.
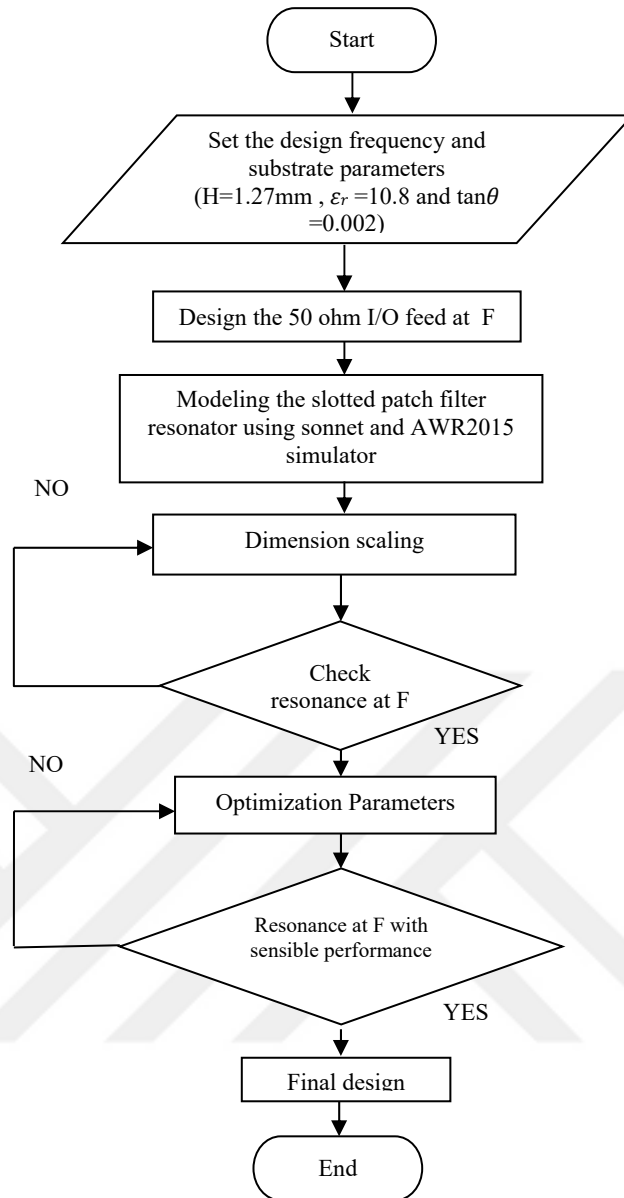
Figure 17: Flowchart for proposed filter designs.

3.2 Filter Design

The essential theory for a microstrip filter modelling is the required properties of the whole categories of resonant modes. At present, microstrip filters design mostly focuses on dual-mode (doubly tuned circuits) structures. Nevertheless, the upper modes have not enough practical realizations. Currently, patch and loop microstrip resonators [1,9] in different forms, hold the vast attention of microwave circuit manufacturers for fabricating new microwave devices and enhancing the frequency responses. A microstrip doubly tuned resonator classically has planar or two-dimensional (2-D) symmetry for different topologies. Figure 1 illustrates some instances of microstrip doubly tuned resonator, where D on top of all resonators in

this illustration points to its regular dimension, and λ_{go} stands for the guided-wavelength at its specified resonance. A miniature patch or slit as induction and coupling element has been placed to each resonator at 45° above the x-axis as shown in Figure 18.
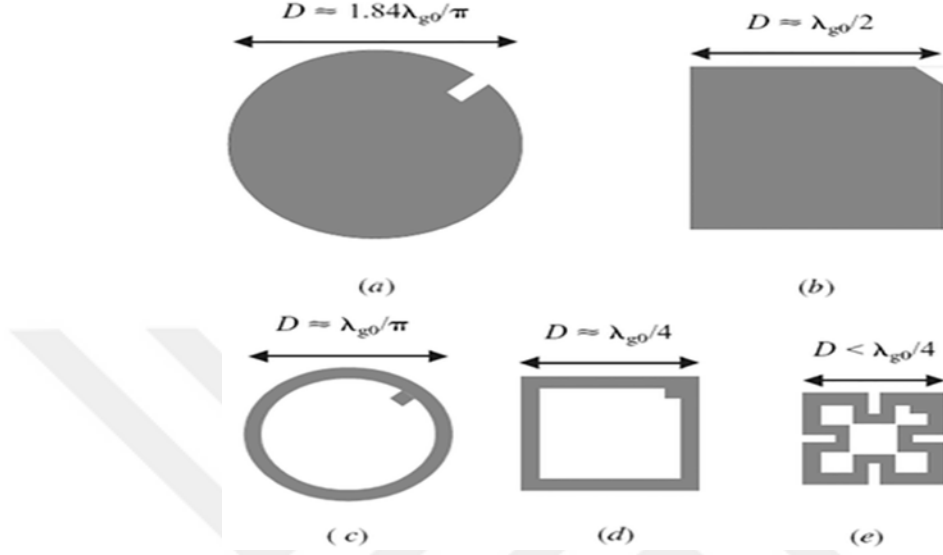
Figure 18: Dual-mode microstrip resonators.

The proposed filters have been simulated by Advanced Wave Research version 12 (AWR12) simulator using dielectric constant of 10.8, dielectric thickness of 1.27 mm and conductor thickness of 35 μm. The guided wave length (λ_{go}) can be evaluated by:

$$\lambda_{go} = \frac{c}{f_0\sqrt{\varepsilon_{eff}}} \tag{4.1}$$

Where c stands for light speed, f_0 is center frequency and ε_{eff} is effective dielectric constant that is roughly calculated as reported in [5] by:

$$\varepsilon_{eff} = \frac{\varepsilon_r + 1}{2} \tag{4.2}$$

Where ε_r stands for relative substrate constant. Eq.(1) is very helpful to correspond to the size of microstrip filter in terms of λ_{go} in order to compare clearly the smallness of diverse filter topologies irrespective of their operating frequency, type of substrate material and external dimensions.

In this study, the filters have been considered as quasi fractal devices since the used resonator has self-similarity and uniform slots like fractals as well as the topology of resonator is newly investigated in this study that let us to refer it as quasi-fractal resonator. The nature of quasi fractal resonator stands for active perturbation effect to the electromagnetic equilibrium of the resonator configuration. Hence, the electromagnetic distributions of the degenerated modes are going to be no longer orthogonal and combined to each other.

Two orthogonal feeds in input and output sides of quasi fractal resonator have been used in BPF design. On the other hand, I/O straight line feed has been adopted in BSF of this study. All feeds have 50 Ohm impedance as standard in filter construction. It is also essential to describe the electromagnetic coupling of quasi fractal resonator with the feed circuit.

The modelled quasi fractal BPF is illustrated in Figure 19. It has been chosen as the finest suitable results by many trials as shown in Table 3.

Table 3: Some Trial examples of BPFs topologies to select the optimal frequency response using RT/Duriod 6010 lm substrate.
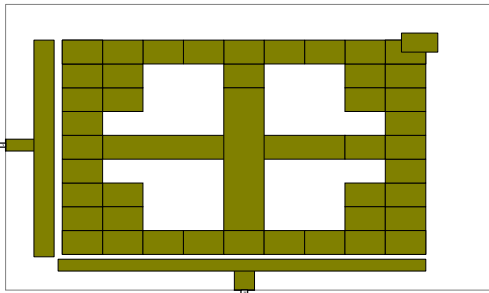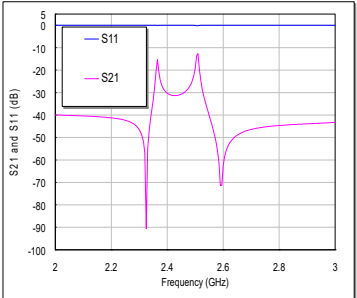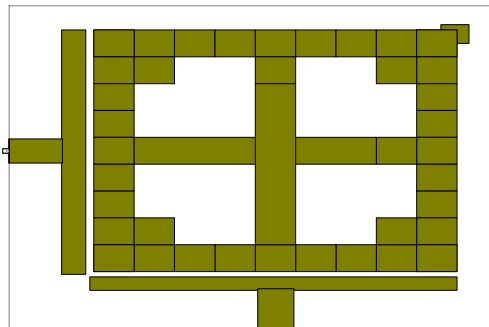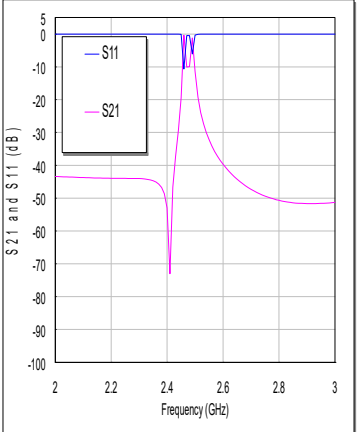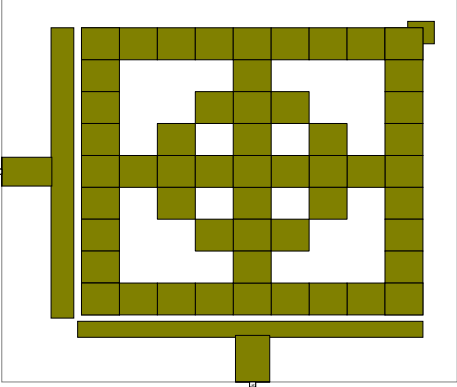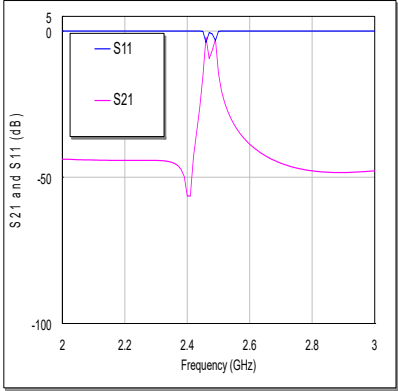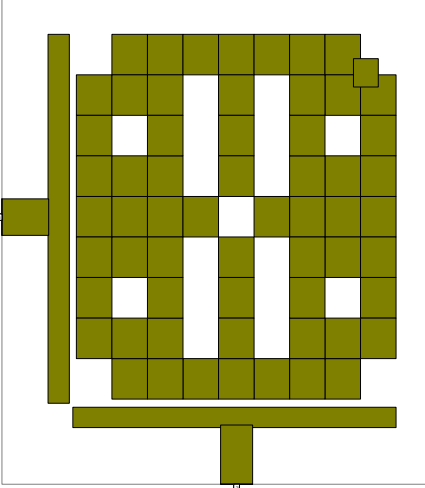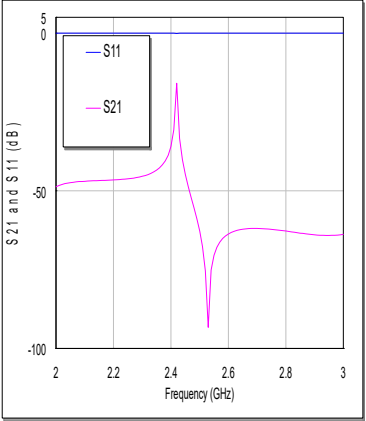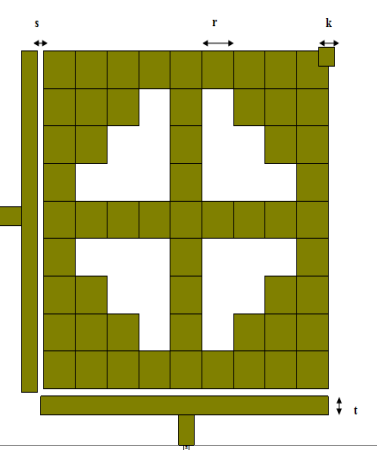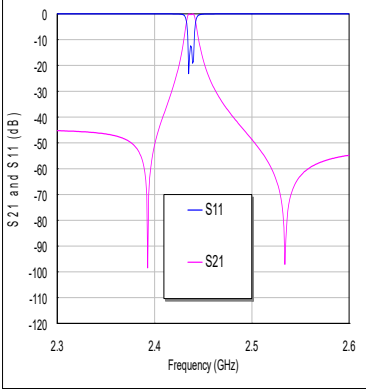
	Filter Shape	Responses
Trial 1		
Trial 2		

Trial 3		
Trial 4		
Trial 5		

It has been constructed using dual-mode patch resonator with regular slots and perturbation element representing by small square patch on the right up corner of quasi fractal resonator. Consequently, this microstrip filter represents two-pole topologies in single structure due to degenerated electromagnetic modes of employed resonator. The perturbation square patch side length (k) is 1 mm while the spacing (s)

among slotted patch resonator and I/O feeds is 0.4 mm and I/O feeder width (t) is 1mm. The length of r that can be used easily to generate quasi fractal resonator is 2 mm. Consequently, the external length of quasi fractal resonator as slotted patch topology is 18 mm. The overall substrate size in this designed BPF is 24 x 24 mm^2.
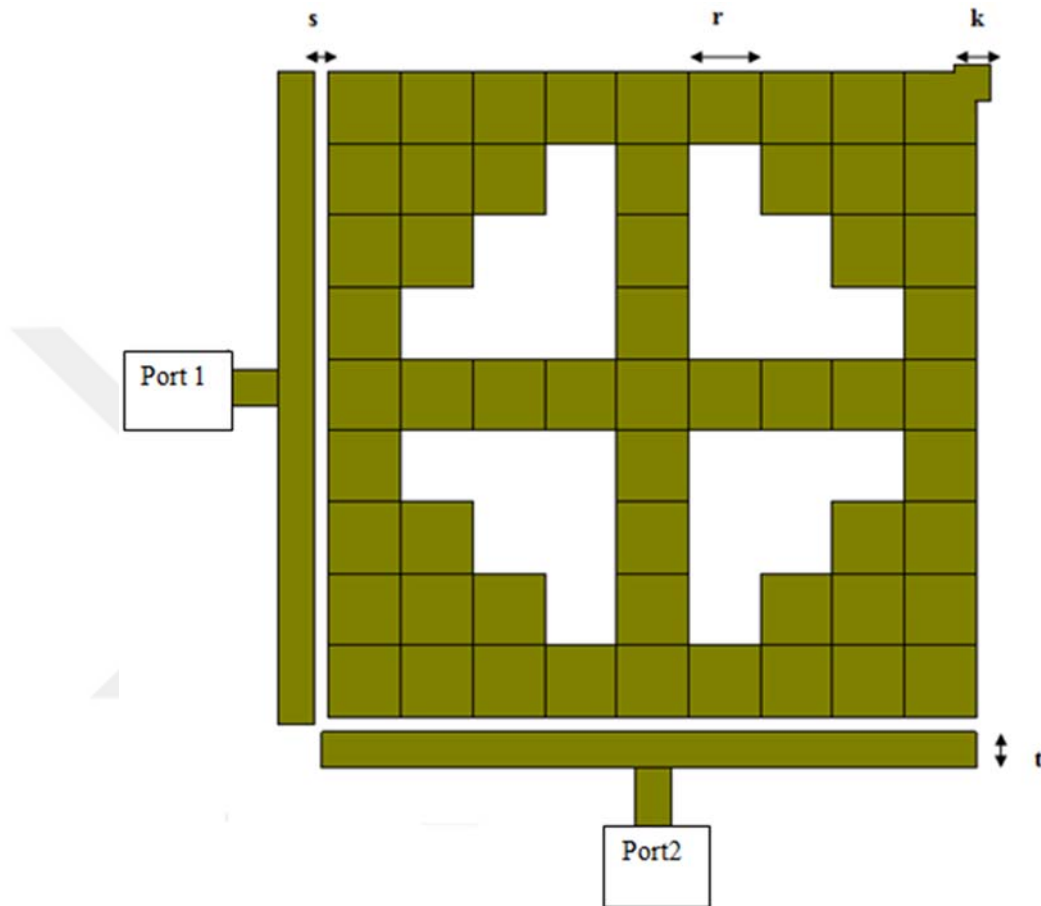
Figure 19: Quasi fractal dual-mode bandpass filter.

By using the same quasi fractal resonator, multi band bandstop filter has been designed as shown in Figure 20 using the same external dimensions, coupling gap and substrate specifications but with using straight line I/O feed of 24 mm length.
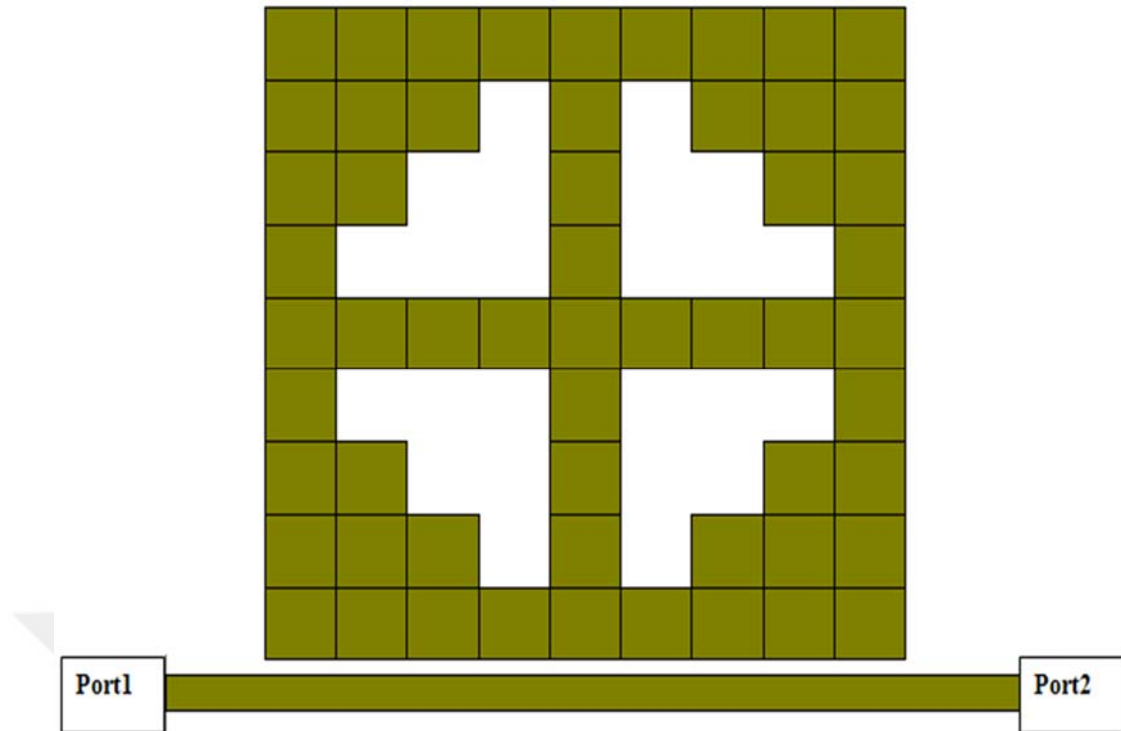
Figure 20: Quasi fractal dual-mode multi bandstop filter.

3.3 Performance Evaluation

Dual degenerate mode microstrip BPF employing quasi fractal resonator is simulated by AWR12 software package. The frequency response for depicted quasi fractal BPF in Figure 19 is shown in Figure 21. The return loss and insertion loss values are -12.426 and -0.2416 dB respectively at centre frequency of 2.437. Dual transmission poles at 2.435 and 2.4392 GHz in the -3dB passband region can be detected noticeably. It is apparent from this graph that there are two transmission zeros that correspond to band stop levels at 2.393 and 2.534 GHz can be observed distinctly with attenuation poles of-98.518 and -97.122. Regarding S_{12} response, it has the same S_{21} response since the topology of filter has self similarity.

This filter has very narrow bandwidth of 9.2 MHz which is usually a big goal in wireless systems to cause the filter able prevent the interfering signals working in the neighbouring bands.
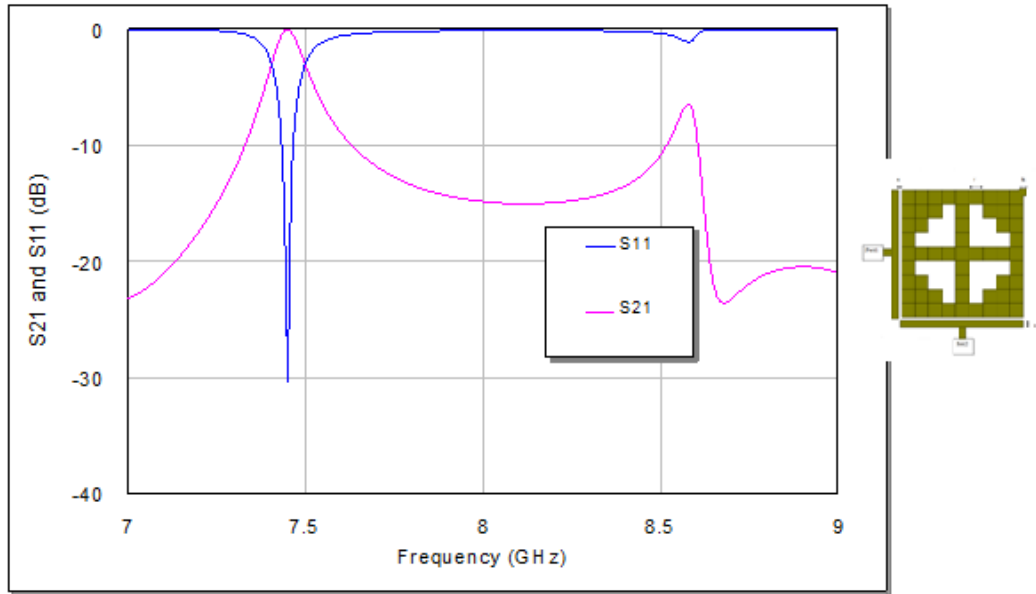
Figure 21: The frequency responses of the microstrip quasi fractal bandpass filter using Fr4 substrate.
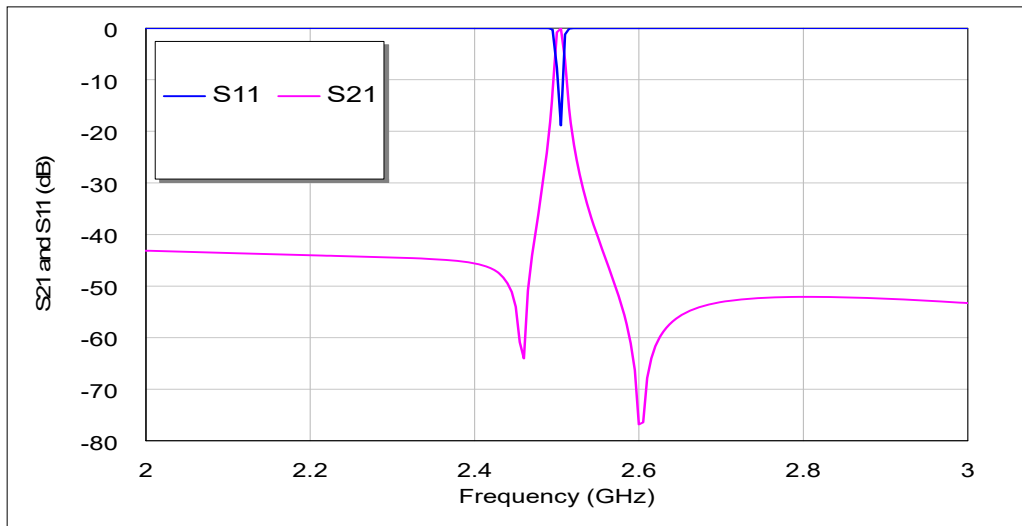

Figure 22: The frequency responses of the microstrip quasi fractal bandpass filter using RT/Duroid 6010.2 lm substrate.

The quasi fractal bandstop filter responses are depicted in Figure 23-24 for FR4 and RT/Duroid 6010.2 lm substrates respectively. The uniform slot of adopted resonator with straight line I/O feeder have EM effects for filter structure to provide a stop band response. For FR4 substrate, the electrical specifications for this band are -0.085 dB return loss, -17.102 dB insertion loss and 63.8 MHz bandwidth at -3dB region at 6.02 GHz, within 5 to 8 GHz sweeping frequency range as depicted in Figure 23. This filter is very useful in broadband wireless schemes which are susceptible to fixed frequency interferences for multi service applications of C band

35

wireless systems. While for RT/Duroid 6010.2 lm substrate frequency response in Figure 24, the electrical specifications for first band are -1.8736 dB return loss, -19.183 dB insertion loss and 40.8 MHz bandwidth at 2.5 GHz. For second band, the results are -0.076 dB return loss, -17.593 dB insertion loss and 34 MHz bandwidth at 4.14 GHz. Lastly, the last appeared band within 2-6 GHz frequency range, the electrical specifications are -1.13 dB return loss, -18.196 dB insertion loss and 46.4 MHz bandwidth at 5.79 GHz.
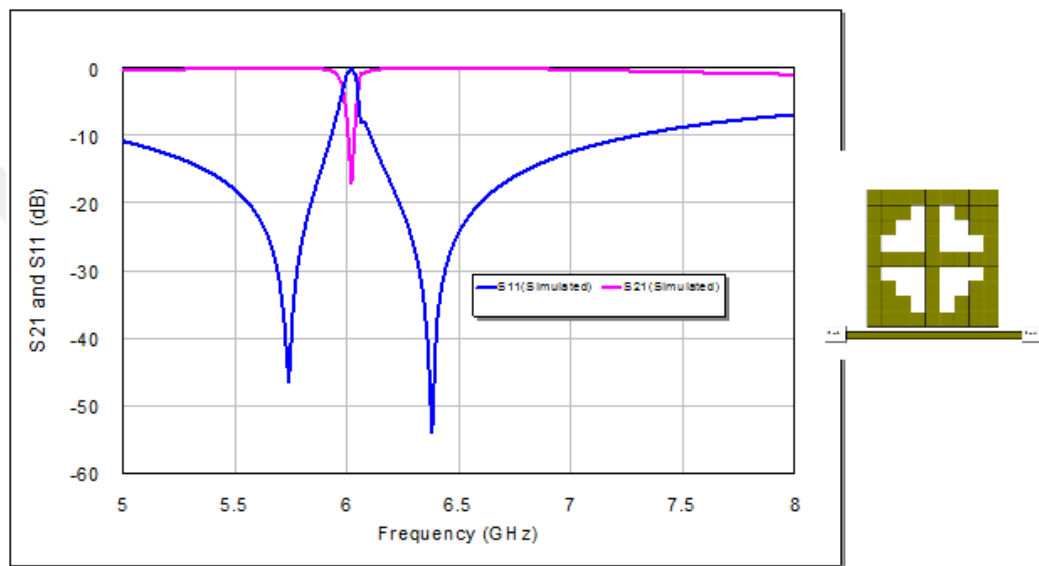
Figure 23: The frequency response of multi bandstop quasi fractal filter for FR4 substrate.
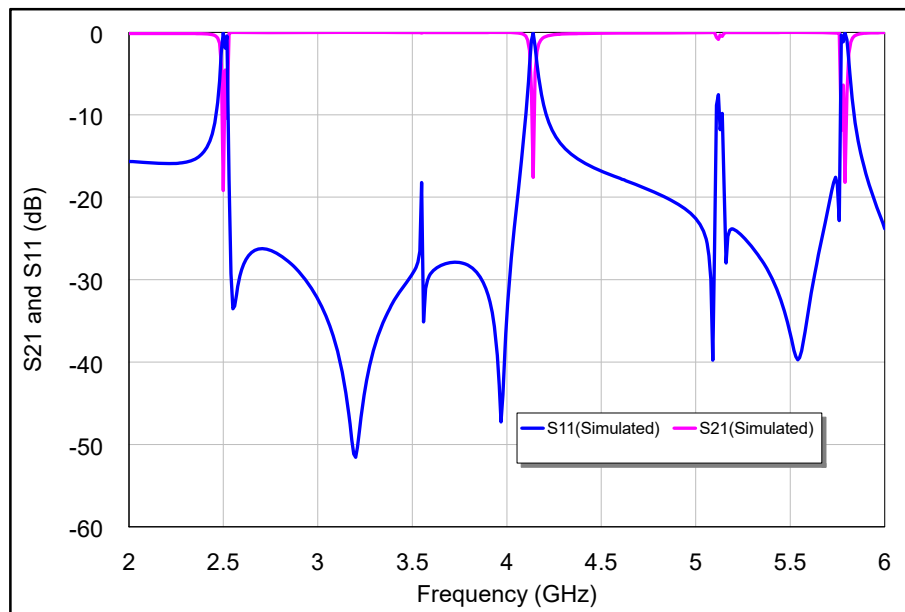

Figure 24: The frequency response of multi bandstop quasi fractal filter for RT/Duroid 6010.2 lm substrate.

Figures 25-28 give an idea about the scattering phase response of the modelled filters for S_{11} and S_{21} parameters respectively. All of them have good level of phase response linearity which is the feature of quasi elliptic filters [17]. The phase response of quasi fractal BPFhas higher jumping levels than quasi fractal BSF.
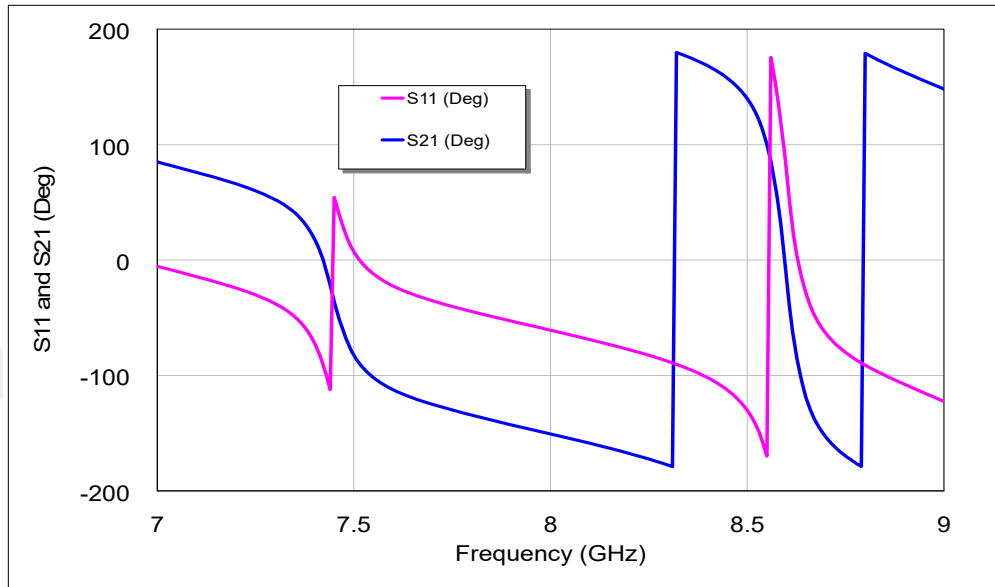

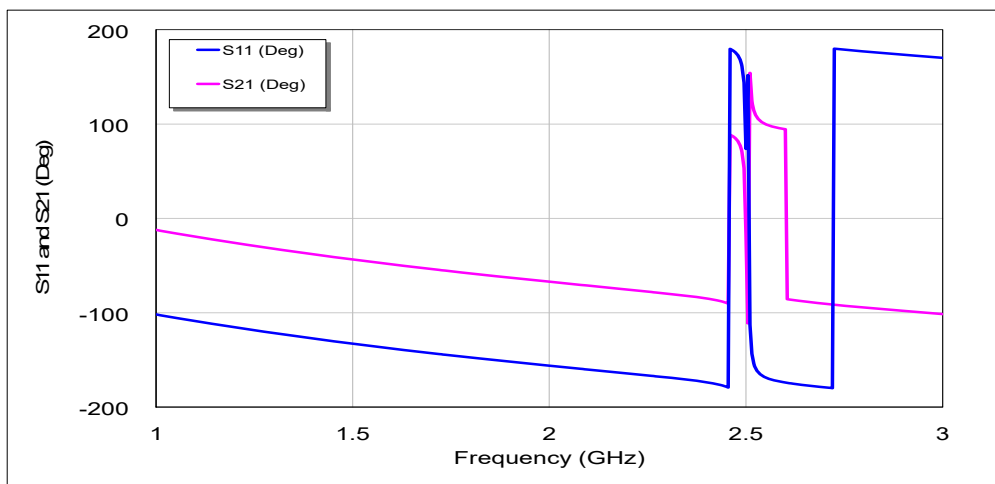**Figure 25:** $S_{21}$and S_{11} phase responses of quasi fractal bandpass filter using FR4 substrate.

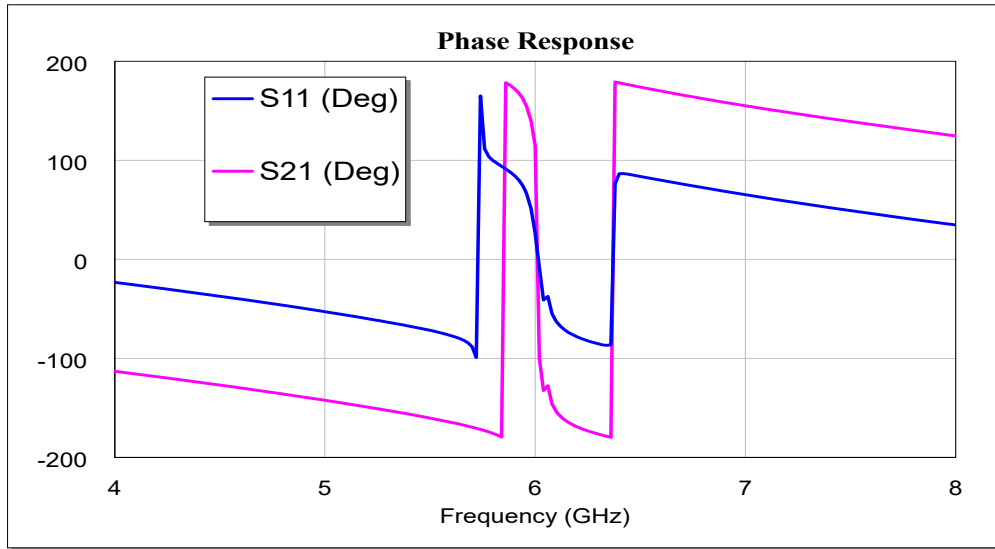**Figure 26:** $S_{21}$and S_{11} phase responses of quasi fractal bandpass filter using RT/Duroid 6010.2 substrate.

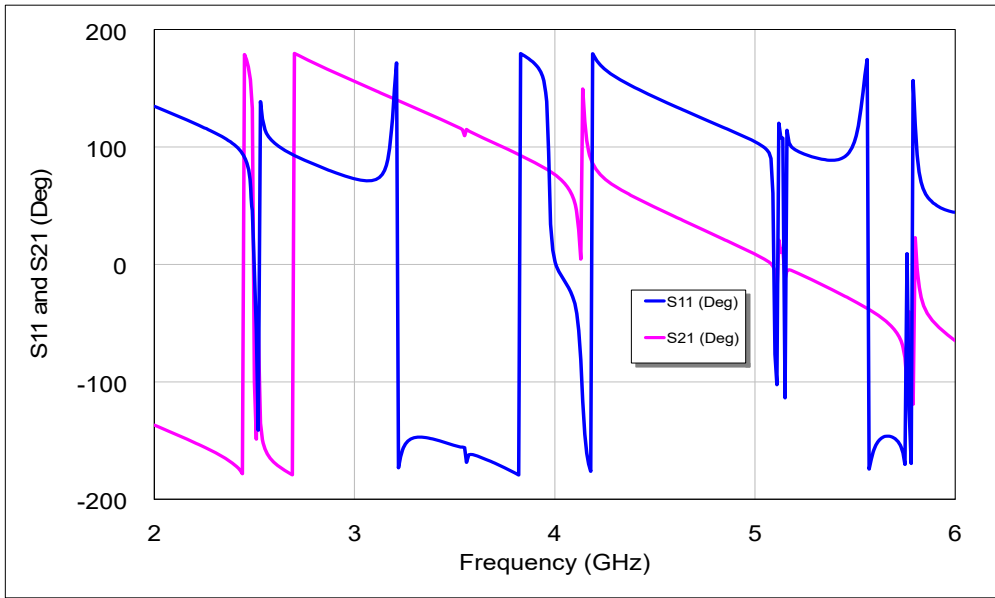**Figure 27:** S_{21} and S_{11} phase responses of quasi fractal bandstop filter using FR4 substrate.

Figure 28: S_{21} and S_{11} phase responses of quasi fractal multi bandstop filter using RT/Duroid 6010.2 lm substrate.

For both substrates, the surface current density simulation results at 7.45 and 2.505 regarding quasi fractal BPF as well as at 6.02 and 2.5 GHz for quasi fractal BSF, have been demonstrated in Figures 29-32 respectively which have the shape of adopted quasi fractal filters. These responses are achieved using Sonnet EM simulator in units of Amp/meter only based on the possibility of this simulator. Units of Volt/meter is not built in Sonnet EM simulator. Based on [16,17,18], the surface current intensity in units of Amp/meter is useful to study the nature of coupling distributions in microstrip filters. In these figures, the red colour is a sign of the

upper limit of coupling whereas the blue colour explains the minimum one. The largest values of surface current intensity are visible in quasi BPF structure for both substrates with magnetic intensity of 11 and 70 Amp/ Meter and that are mostly distributed centrally and symmetrically in all segments of designed quasi fractal BPF. On the other hand, the maximum current intensity for quasi fractal BSF for both substrates is 4.2 and 6.9 Amp/ Meter which are distributed mostly in the straight I/O feed of BSF.
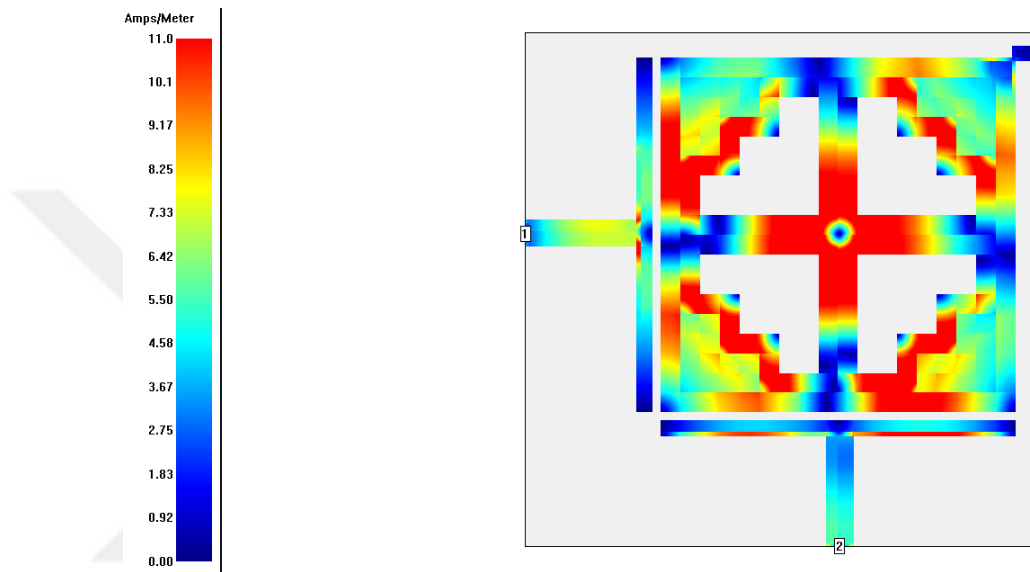

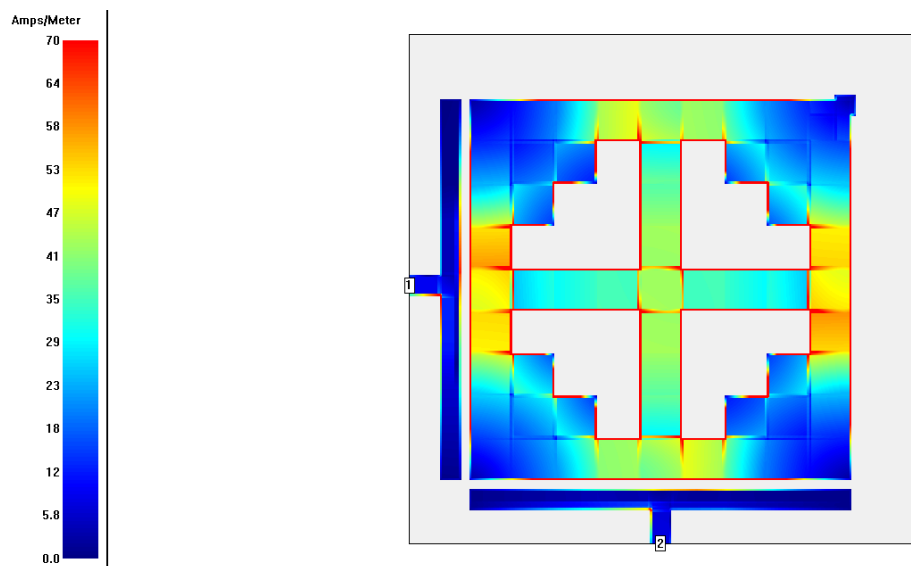**Figure 29:** Current intensity distributions of quasi fractal BPF at 7.45 GHz for FR4 substrate.

Figure 30: Current intensity distributions of quasi fractal BPF at 2.5 GHz for RT/Duroid 6010.2 lm substrate.
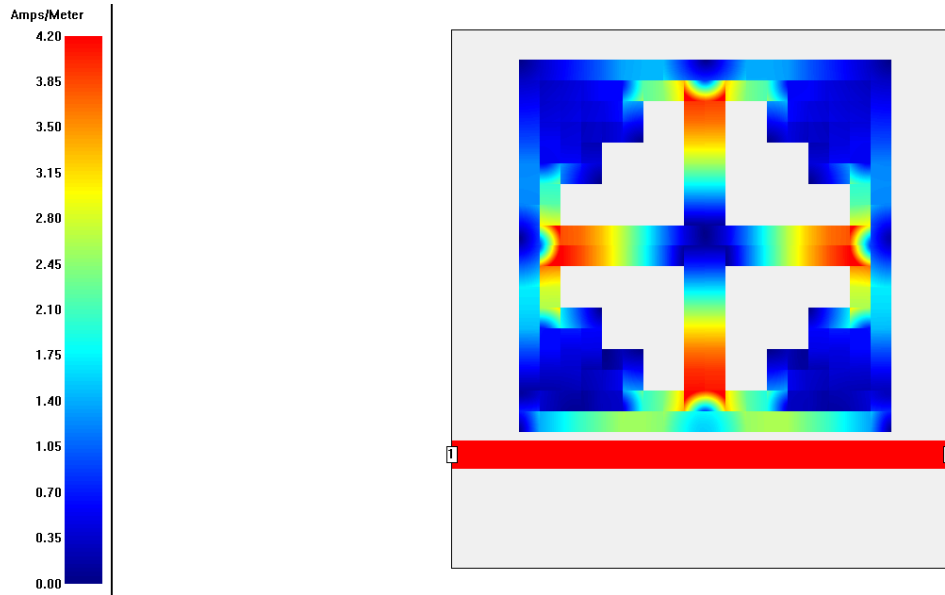
Figure 31: Current intensity distributions of quasi fractal BSF at 6.02 GHz for FR4 substrate.
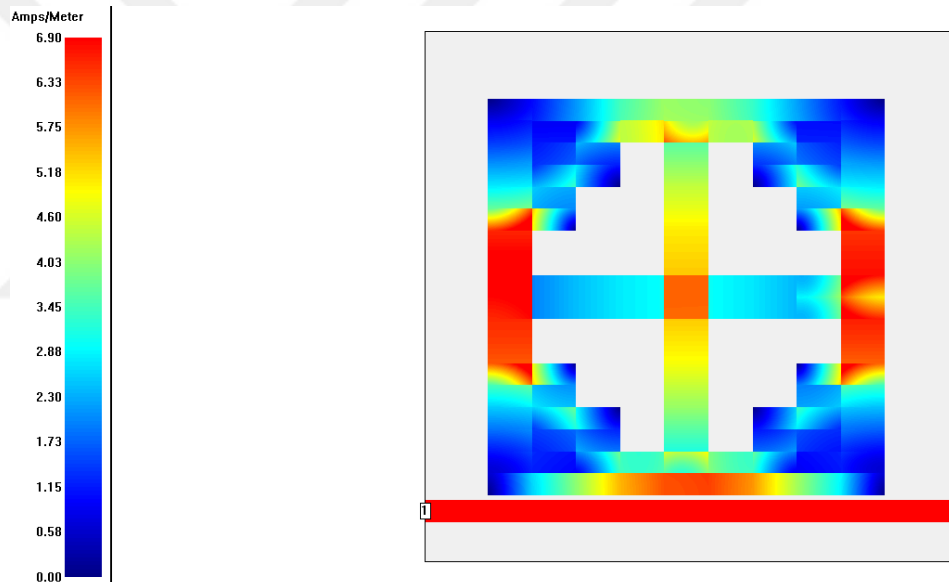

Figure 32: Current intensity distributions of quasi fractal BSF at 2.5 GHz for RT/Duroid 6010.2 lm substrate.

Theoretically, very narrow microstrip BPF that has fractional bandwidth less than 1 %is very rare, but in HTS filters is possible [24]. However, HTS filters require efficient coolers to decrease the resultant heat due to narrow strips of HTS topology. This, of course, decreases the compactness benefit of this type of filters. The proposed microstrip BPF in this study has interesting compactness and very narrow passband response of 1.25 and 0.419 %fractional bandwidth for FR4 and RT/Duroid 6010.2 lm respectively. These very narrow bandwidths are very purposeful in wireless systems in excluding interfering signals in adjacent bands and increases

hugely the external quality factor of designed filter. On the other hand, the designed bandstop filter has narrow reject band peak that can be useful for wireless system applications that require wide passband responses with narrow reject band separations as in similar bandstop filter applications reported in [17, 25].

Figures 33and 34 show the prototype photographs of quasi fractal BPFs using FR4 and RT/Duroid 6010.2 lm substrates respectively. Quasi fractal resonator are printed on FR4 substrate using the standard mask etching technique. Figures 34 and 35 illustrate the experimental and simulated frequency responses of these fabricated filters using the both substrates. The measurements of these prototypes are prepared using Anristu MS4642A vector network analyzer using 50 Ohm feeds. On the other hand, Figures 36 and 37 show the prototype photographs of quasi fractal BSFs using FR4 and RT/Duroid 6010.2 lm substrates respectively. The experimental and simulated frequency responses of these fabricated filters using the both substrates are shown in Figures 38-39. The measurements of these prototypes are prepared using Agilent vector network analyzer. Both simulations and measurements for all designed filters in this study are in good agreement with acceptable differences. These differences are attributed to fabrication tolerances, simulation accuracy connector soldering, and cables losses.

Figure 33: Photograph of the fabricated quasi fractal BPF using FR4 substrate.
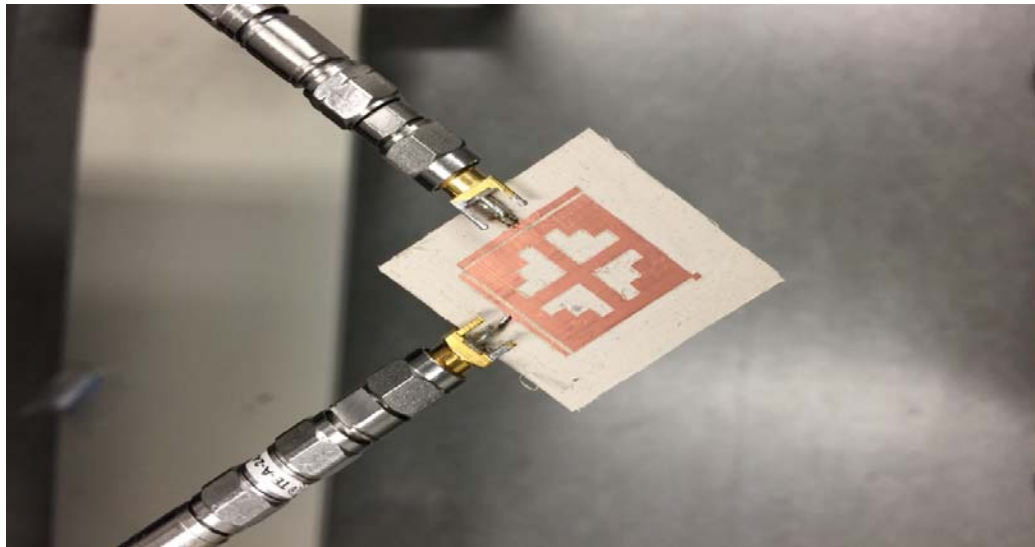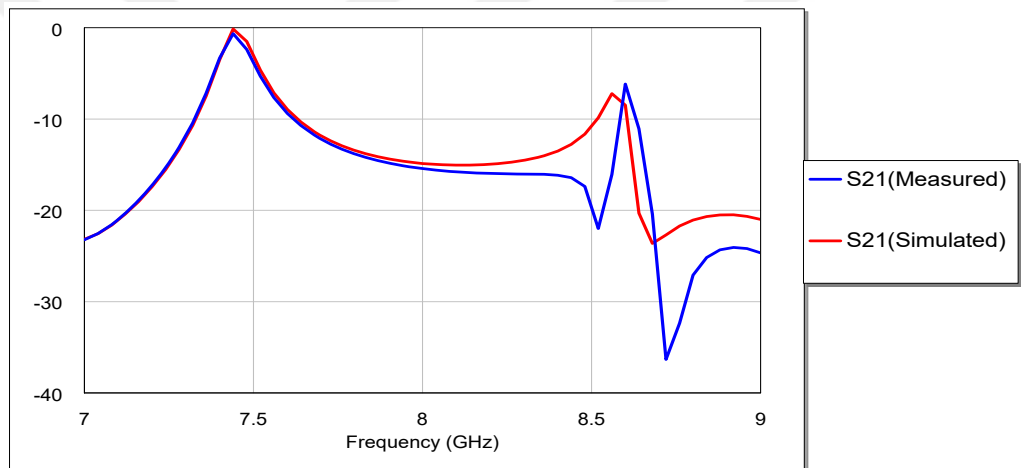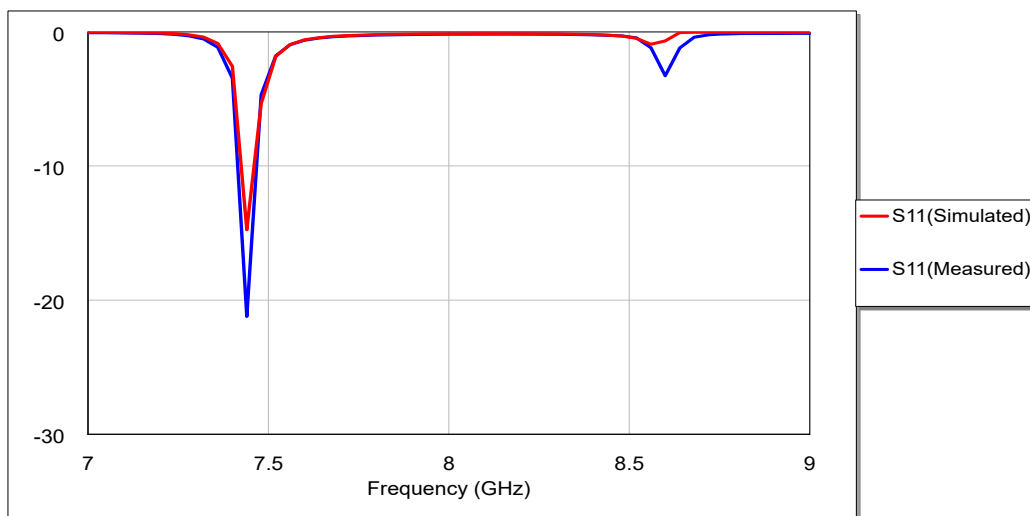
Figure 34: Photograph of the fabricated quasi fractal BPF using RT/Duroid 6010.2 lm substrate.

(a) S_{21}

(b) S_{11}

Figure 35: Simulated and measured frequency responses of designed quasi fractal BPF using FR4 substrate.

(a) S_{21}

(b) S_{11}

Figure 36: Simulated and measured frequency responses of designed quasi fractal BPF using RT/Duroid 6010. 2 lm substrate.

Figure 37: Photograph of the fabricated quasi fractal BSF using FR4 substrate.

Figure 38: Photograph of the fabricated quasi fractal BSF using RT/Duroid 6010.2 lm substrate.

(a) S_{11}

(b) S_{21}

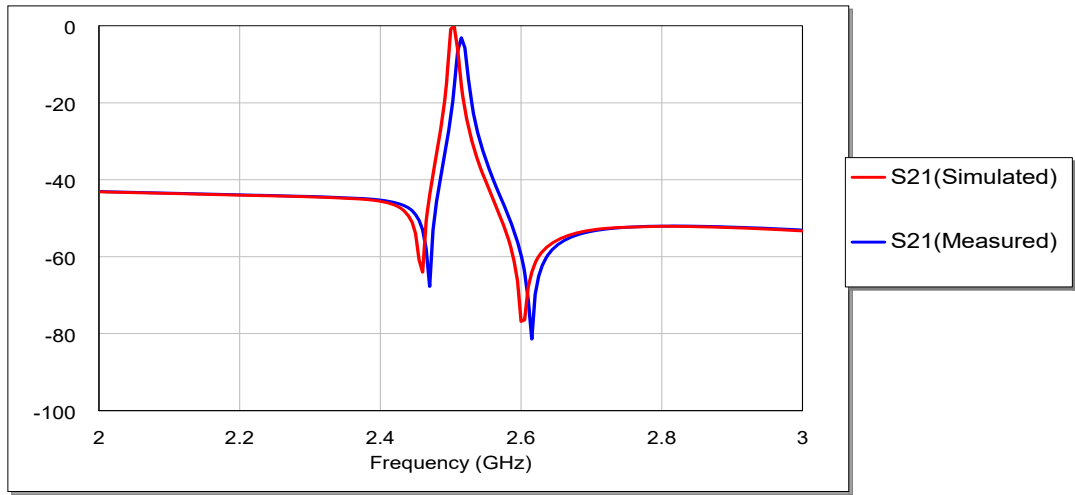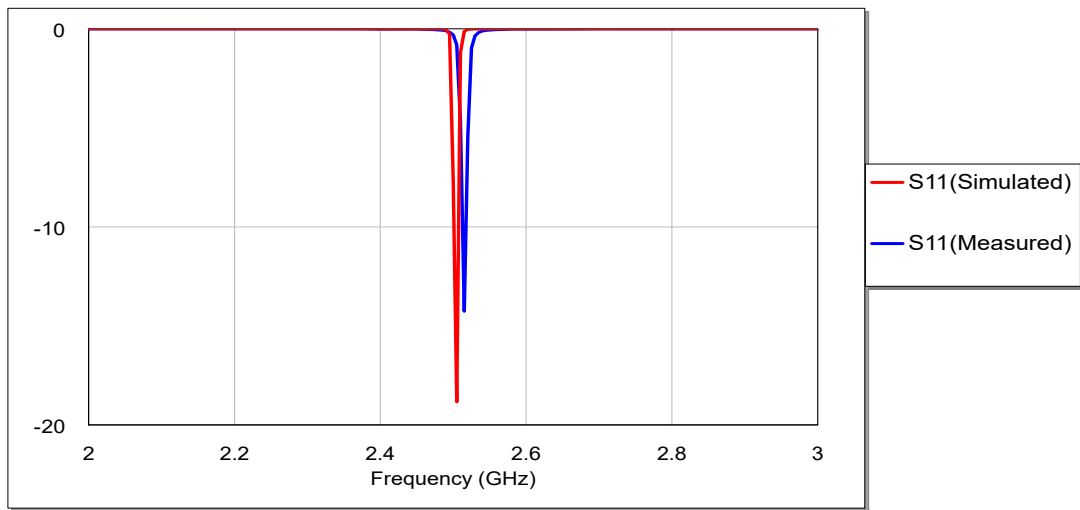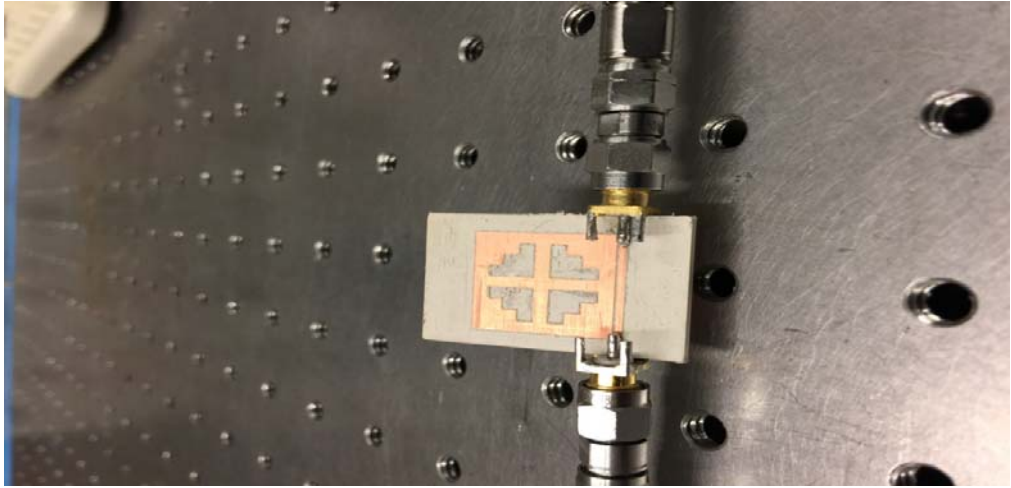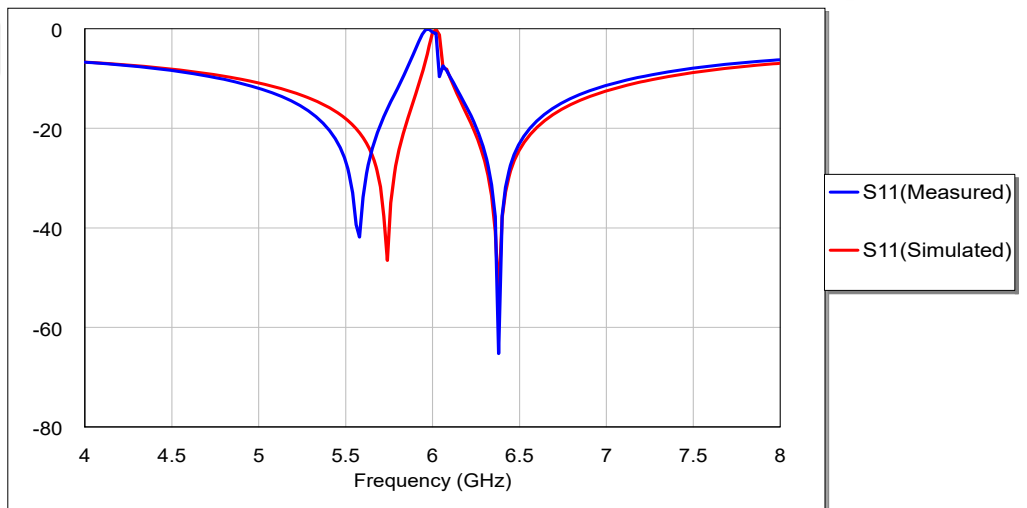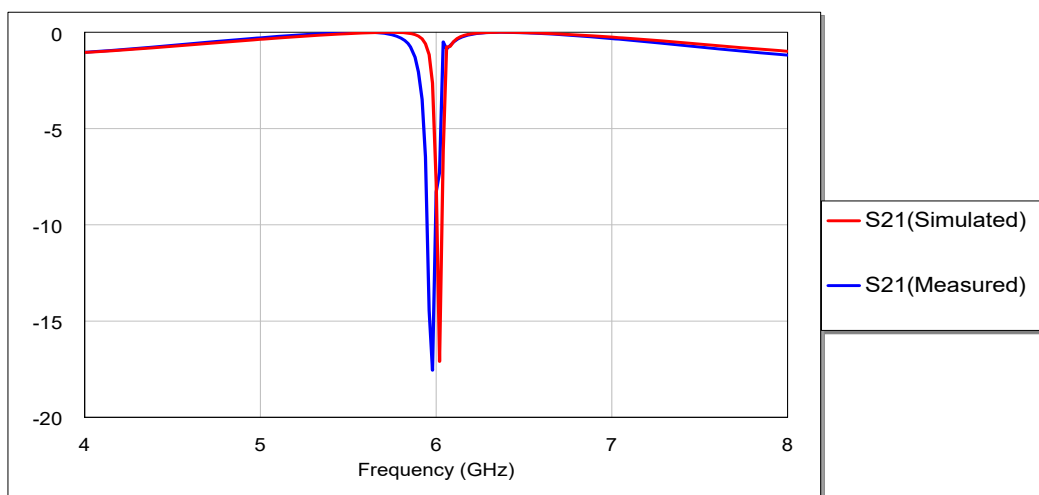**Figure 39:** Simulated and measured frequency responses of designed quasi fractal BSF using FR4 substrate.
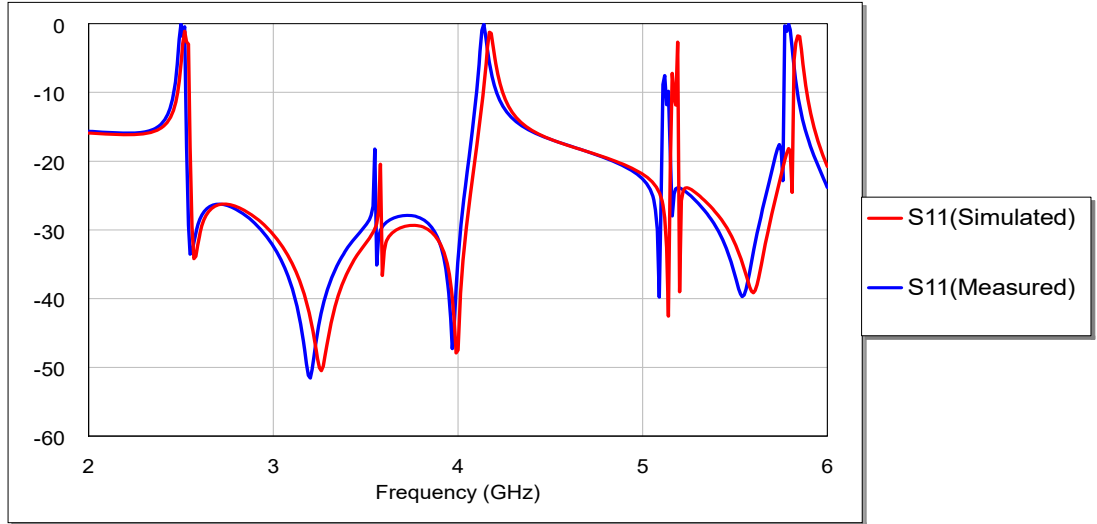
(a) S_{11}
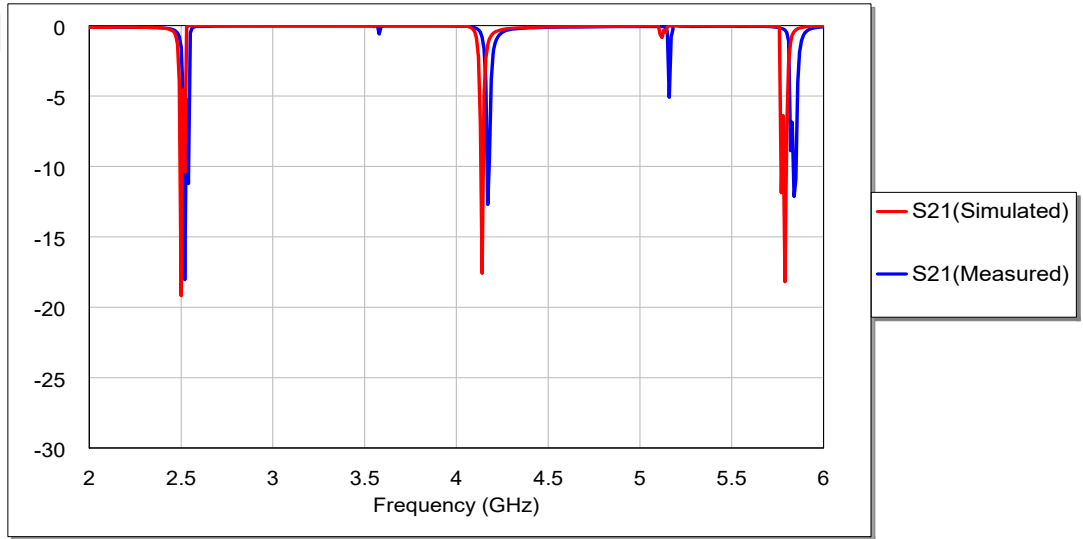
(b) S_{21}

Figure 40: Simulated and measured frequency responses of designed quasi fractal BSF using RT/Duroid 6010.2 lm substrate.

The shift in operating frequency between FR4 and RT/Duroid6010.2 micrstrip filters are due to change in dielectric permittivity (ε) for both substrates which is inversely proportional to the resultant capacitance (C) and hence inversely proportional to the resonant frequency (f_0)as it is clear from (4.1) and (4.2) in the constancy of area (A) and substrate thickness (d) and lumped inductance (L).

$$C= \varepsilon \; \frac{A}{d} \qquad\qquad (4.1)$$

$$f_0 = \frac{1}{\sqrt{LC}} \qquad\qquad (4.2)$$

In addition to considerable compactness of filter due to small surface area as well as noticeable smallness in terms of guided wavelength, the proposed quasi

fractal BPF using FR4 substrate in this study has the narrowest fractional bandwidth, the best external quality factor than reported filter in [26] used for C band wireless applications as illustrated in Table 4. On the other hand, the projected quasi fractal BPF using RT/Duroid 6010.2 lm substrate has the narrowest fractional bandwidth, the best external quality factor and totally or almost better electrical filter specifications in terms of return loss and insertion loss than reported filters in [12, 27-32] used for wireless applications as illustrated in Table 5.

Table 4: Comparison of the designed dual-mode BPF with [26] around 7.4 GHz for wireless C band application.
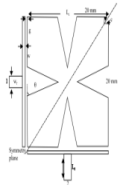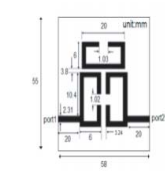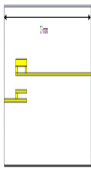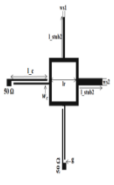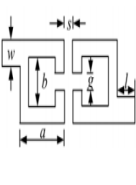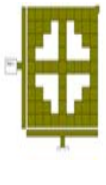
Filter Parameters	[26]	Quasi fractal BPF in this study
Centre Frequency(GHz)	7.4	7.45
Dielectric Constant and Thickness	4.4, 1.5 mm	10.8, 1.27 mm
Size (mm^3)	24X 8X 4.5	24 x 24X1.5
Bandwidth(MHz)	160	93.3
Fractional Bandwidth (%)	2.16	1.25
External Quality Factor (Qext)	92.5	160
Measurement	Centre frequency=7.42 GHz, return loss=-15 dB, insertion loss = better than -1 dB	Centre frequency=7.4 GHz, return loss=-21 dB, insertion loss = better than -3 dB
Filter Shape in Simulated		

Table 5: Comparison of the designed dual-mode BPF of RT/Duroid substrate with [12, 27-32].

Filter Parameters	[12] for 1st iteration structure	[27]	[28]	[29]	[30]	[31]	[32]	Dual mode BPF in this study
Center Frequency(GHz)	2.4	2.4	2.4	2.4	2.44	2.44	2.44	2.505
Insertion Loss(dB),S21	-0.901	-0.3	-8.15	-1	-1.25	-2.5	3	-0.057
Return Loss(dB),S11	-7.25	-16.5	-35	-20	-25	-15	15	-18.841
Dielectric Constant and Thickness	10.8, 1.27 mm	2.2, 31 mil	4.4, 1.6 mm	3.55, 0.813	2.55, 1 mm	4.41. 1.6 mm	3.38, 0.508 mm	10.2, 1.27 mm
Size (mm^2)	23.214 x 23.214	58 x 58	23 x 12	57 x 57	....	....	17 x 9	24 x 24
Size byλ_{go}^{2}	$0.451\lambda_{go}$ x $0451\lambda_{go}$	$0.587\lambda_{go}$ x $0.587\lambda_{go}$	$0.302\lambda_{go}$ x $0.158\lambda_{go}$	$0.688 \lambda_{go}$ x $0.888\lambda_{go}$	....	....	$0.2\lambda_{go}$ x $0.08\lambda_{go}$	$0.474\lambda_{go}$ x $0.474\lambda_{go}$
Bandwidth(MHz)	30	25	130	1400	200	146.4	80	10.5
Fractional Bandwith (%)	1.25	1.04	5.42	58.33	8.2	6	3.28	0.419
External Quality Factor (Qext)	160	192	36.92	3.43	24.4	3.33	61	477.14
Measurement	………..	Centre frequency =2.417 GHz Return loss is about -17 dB and insertion loss is -3.5 dB	………..	Centre frequency =2.417 GHz Return loss is about -17 dB and insertion loss is -3.5 dB	Centre frequency =2.44 GHz Return loss is about -20 dB and insertion loss is -0.73 dB	Centre frequency =2.44 GHz Return loss is about -15 dB and insertion loss is -2.5 dB	Centre frequency =2.44 GHz Return loss is better than --15 dB and insertion loss is about -5 dB	Centre frequency =2.55 GHz Return loss is about --15 dB and insertion loss is better than -3 dB
Filter Shape in Simulated								

CHAPTER FIVE

CONCLUSION AND SUGGESTION FOR FUTURE WORK

In this study, microstrip BPF and BSF filters have been presented. The proposed filters employ slotted patch microstrip resonator based on quasi fractal geometry, simulated by AWR_{12} software package. For FR4 substrate, the proposed quasi fractal BPF is designed at centre frequency of 7.45 GHz, while quasi fractal BSF is designed at band frequencies of 6.02 GHz respectively. The presented quasi fractal BPF has extremely narrow fractional bandwidth of 1.25%, which is theoretically extraordinary in microstrip filter design. On the other hand, quasi fractal BSF can be integrated with in broad band wireless systems that are receptive to permanent frequency interferences for C band wireless applications. The measured frequency responses are in adequate performances. For RT/Duroid 6010.2 lm substrate, the projected quasi fractal BPF is designed at centre frequency of 2.505 GHz, while quasi fractal multi band BSF is designed at band frequencies of 2.5, 4.14 and 5.79 GHz respectively. The presented quasi fractal BPF has extremely narrow fractional bandwidth of 0.419%, which is tentatively amazing and ultra narrow band in microstrip filter design. On the other hand, quasi fractal BSF can be integrated with in broad band wireless systems that are receptive to permanent frequency interferences for ISM and C band wireless applications. The measured frequency responses are in good agreement with the simulations.

The field of producing miniaturized BPFs and BSFs for different wireless communication systems, using the fractal or quasi fractal concepts is still slowly

1. Based on the findings and gained results of this study, supplementary researches should be conducted to inspect the possibility of realizing more miniature dual-mode quasi fractal filters using SIR techniques or meandering process.

2. Make use of the compact size satisfied in this work to design smaller band response BPFs and BSFs with higher number of poles. These types of filter with narrower and sharper responses are needed in many wireless systems working with adjacent bands to prevent interference.

3. Using hybrid fractal geometries or defected ground structure (DGS) technique to produce promising compacted filter topologies with interesting frequency responses.

4. Mate-materials can be also adopted with quasi fractal filters with advanced performance as future feasible studies.

5. Investigation of applying multi layer substrate with quasi fractal or fractal geometries to produce dual/ multi-band filters for recent telecommunication schemes.

REFERENCES

[1]   J.S. Hong and M.J. Lancaster (2001), Microstrip Filters for RF/Microwave Applications, John Wiley & Sons.

[2]   Shahd k. Khaleel, "Design and Simulation of Diplexers for Wireless Communication Systems", M.Sc Thesis, University of Technology, Iraq, 2016.

[3]   J. S. Hong and M. J. Lancaster (1996), Compact Microwave Elliptic Function Filter Using Novel Microstrip Meander Open-Loop Resonators, Electronics Letters, vol. 32, no. 6, pp. 563–564.

[4]   D. M. Pozar, "Microwave Engineering", John Wiley & Sons, Inc.,2012.

[5]   Y.S. Mezaal, H.T. Eyyuboglu and J.K. Ali, "'New Dual Band Dual-Mode Microstrip Patch Bandpass Filter Designs Based on Sierpinski Fractal Geometry", Proceeding of Advanced Computing and Communication Technologies, pp. 348-352, 2013.

[6]   J. Romeu and J. Soler, "Generalized Sierpinski fractal multiband antenna," IEEE Transactions on Antennas and Propagation, vol. 49, no. 8, pp. 1237 – 1239, Aug. 2001.

[7]   B. B. Mandelbrot, "The Fractal Geometry of Nature," New York, W. H. Freeman, 1983.

[8]   O. I. Yordanov, I. Angelov, V.V. Konotop and I.V. Yurkevich "Prospects of Fractal Filters and Reflectors," in IEE Seventh International Conference on Antenna and Propagation ISCAP'91, pp. 698-700, York, UK, 1991.

[9]   M. Barra. "Miniaturized Superconducting Planar Filters for Telecommunication Applications", PhD Thesis, University of Napoli, Italy, 2004.

[10] J.K. Ali, "A New Miniaturized Fractal Bandpass Filter Based on Dual-Mode Microstrip Square Ring Resonator," *Proceedings of the 5th International Multi-Conference on Signals, Systems and Devices, IEEE SSD '08,* Amman, Jordan, July 20-23,2008.

[11] Y.S. Mezaal, "A New Microstrip Bandpass Filter Design Based on Hilbert Fractal Geometry for Modern Wireless Communication Applications," *International Journal on advanced Computing Techniques, IJACT*, vol.1, no.2, pp.36-39, 2009.

[12] Ahmed A. Mahdi and Jabir S. Aziz, Miniaturized Koch Pre-Fractal Bandpass Filter, Journal of Mobile Communication 5 (5-6): 57-61,2011.

[13] J. K. Ali, and Y. S. Mezaal, "A New Miniature Narrowband Microstrip Bandpass Filter Design Based on Peano Fractal Geometry," Iraqi Journal of Applied Physics, vol. 5, no. 4, pp. 3-9, 2009.

[14] J. K. Ali, and Y. S. Mezaal,"A new miniature fractal-based bandpass filter design with 2nd harmonic suppression," Proceedings of 3rd IEEE International Symposium on Microwave, Antenna, Propagation and EMC Technologies for Wireless Communication, *MAPE 2009*.

[15] J. K. Ali, Hussam Alsaedi, Mohammed F. Hasan, and Hussain A. Hammas, "A Peano fractal-based dual-mode microstrip bandpass filters for wireless communication systems." In *PIERS Proceedings*, pp. 888-892. 2012.

[16] Mezaal, Y. S., Jawad K. Ali, and H. T. Eyyuboglu. "Miniaturised microstrip bandpass filters based on Moore fractal geometry." *International Journal of Electronics* 102.8 (2015): 1306-1319.

[17] Y.S. Mezaal, H.T. Eyyuboglu and J.K. Ali (2014) Wide Bandpass and Narrow Bandstop Microstrip Filters Based on Hilbert Fractal Geometry: Design and Simulation Results, PLOS ONE | DOI:10.1371/journal.pone.0115412.

[18] Y.S. Mezaal and H.T. Eyyuboglu (2016) Investigation of New Microstrip Bandpass Filter Based on Patch Resonator with Geometrical Fractal Slot, Plos One 11(4): e0152615. Doi:10.1371/ journal.pone.0152615.

[19] Yaqeen S. Mezaal, New Microstrip Quasi-Fractal Antenna: Design and Simulation Results, 2016 IEEE 36th International Conference on Electronics and Nanotechnology (ELNANO), Kiev,2016.

[20] Fattah Talaei, Mohammad N. Azarmanesh, Gholamreza Askari, and Hamid Mirmohammadsadeghi, "A novel dual-mode dual band bandpass filter using a quasi fractal structure," IEICE Electronics Express, Vol.7, No.3, 153-158, Feb. 2010.

[21] Ghatak, R., R. K. Mishra, D. R. Poddar, and A. Patnaik, "Multilayered complementary quasi-fractal Sierpinski patch antenna for wireless terminals,"

URSI XXVIII GA Poster Presentations Programme, 95, 2005.

[22] Jawad K. Ali, and A. S. A. Jalal, "A Miniaturized Multiband Minkowski-Like Pre-Fractal Patch Antenna for GPS and 3g IMT- 2000 Handsets", Asian Journal of Information Technology 6(5), pp. 584-588, 2007.

[23] F. Viani, " Dual-band Sierpinski Pre-Fractal Antenna for 2.4 GHz- References 117 WLAN and 800 MHz-LTE Wireless Devices ", Progress In Electromagnetics Research C, PIERS, Vol. 35, pp. 63-71, 2013.

[24] D. Zhang, G. C. Liang, C. F. Shih, M. E. Johansson, R. S. Withers, "Narrowband lumped element microstrip filter using capacitively loaded inductors", *IEEE Trans. Microwave Theory Tech.*, vol. 43, pp. 3030-3036, Dec. 1995.

[25] Ahmed, H.S., A.J. Salim, J.K. Ali, and N.N. Hussain. "A Compact Triple Band BSF Design Based on Minkowski Fractal Geometry." 18th IEEE Mediterranean Electrotechnical Conference, MELECON 2016, Limassol, Cyprus, April 2016.

[26] Q.R.Li, et al., Design of a narrowband HTS filter at 7.4-GHz with improved upper-stopband performance, Physica C 483 (2012) 5–7.

[27] Saghlatoon H. and Neshati M. H.: Design Investigation of a Novel Bandpass Filter Using Trisection Open Loop Resonator. Progress In Electromagnetics Research Symposium Proceedings, Malaysia, 1203-1206, (2012).

[28] Chhabra A., Khanna R. and Kumar N.: A Novel Compact Band Pass Filter for 2.4 GHz ISM Band Applications, Indian Journal of Science and Technology, vol. 9(47), DOI: 10.17485/ijst/2016/v9i47/106452, (2016).

[29] Arain S., Abassi Muhammad A. B., Nikolaou S. and Vryonides P.: A Square Ring Resonator Bandpass Filter With Asymmetrically Loaded Open Circuited Stubs. 5th IEEE International Conference on Modern Circuits and Systems Technologies,2016.

[30] Weng, L. H., Guo, Y. C., Chen, X. Q. and Shi, X. W. 2008. Microstrip open loop resonator bandpass filter with DGS for WLAN application. Journal of Electromagnetic Waves and Applications, 22(No. 14–15): 2045–2052.

[31] A. Griol, J. Marti, L. Sempere, "Microstrip multistage coupled ring bandpass filters using spur-line filters for harmonic suppression", *Electron.Lett.*, vol. 37, no. 9, pp. 572-573, Apr. 2001.

[32] Azzeddine Djaiz, and Tayeb A. Denidni, "A Design and Fabrication of a New Stacked Bandpass Filter Using Multilayer Microstrip Structure For Wireless Applications," IEEE Radio and Wireless Conference RAWCON, Boston, USA, pp. 317-320, Aug 2003.

CURRICULUM VITAE

PERSONAL INFORMATION

Surname, Name   : Saleh, Hiba Hashim

Nationality   : Iraqi

Date and Place of Birth : 14.12.1987.IRAG

Phone   : 05369572299

Fax   :

Email   : Hibaeng40@yahoo.com

EDUCATION

Degree	Institution	Year of Graduation
BS	Electric and electronic engineering	2008-2009

WORK EXPERIENCE

Year	Place	Enrolment
2010	REPUBLIC OF IRAQ DIYALA GOVERNORATE	engineer

FOREIGN LANGUAGES

English, Turkish